Svalbard Composite Tectono-Sedimentary Element, Barents Sea

Snorre Olaussen[1]*, Sten-Andreas Grundvåg[1,2], Kim Senger[1], Ingrid Anell[1,3], Peter Betlem[1,3], Thomas Birchall[1,3], Alvar Braathen[1,3], Winfried Dallmann[2], Malte Jochmann[1,4], Erik P. Johannessen[5], Gareth Lord[1], Atle Mørk[6], Per T. Osmundsen[1,6], Aleksandra Smyrak-Sikora[1] and Lars Stemmerik[1,7]

[1]Department of Arctic Geology, University Centre in Svalbard PO Box 156, N-9171, Longyearbyen, Norway

[2]Department of Geosciences, UiT The Arctic University of Norway, PO Box 6050 Langnes, N-9037 Tromsø, Norway

[3]Department of Geosciences, University of Oslo PO Box 1047, Blindern, N-0316 Oslo, Norway

[4]Store Norske Spitsbergen Kulkompani AS PO Box 613, N-9171 Longyearbyen, Norway

[5]EP Skolithos Sisikveien 36, N-4022 Stavanger, Norway

[6]Department of Geoscience and Petroleum, Norwegian University of Science and Technology, N-7491 Trondheim, Norway

[7]Geological Survey of Denmark and Greenland Øster Voldgade 10, DK-1350 Copenhagen K, Denmark

SO, 0000-0002-7922-8010; S-AG, 0000-0002-4309-898X; KS, 0000-0001-5379-4658; PB, 0000-0002-6017-9415; TB, 0000-0002-2252-4687; AB, 0000-0002-0869-249X; MJ, 0000-0001-9386-573X; AM, 0000-0002-0233-224X; AS-S, 0000-0001-9321-1269

*Correspondence: Snorreo@unis.no

Abstract: The Svalbard Composite Tectono-Sedimentary Element (SCTSE) is located on the northwestern corner of the Barents Shelf and comprises a Carboniferous–Pleistocene sedimentary succession. Due to Cenozoic uplift, the succession is subaerially exposed in the Svalbard archipelago. The oldest parts of the succession consist of Carboniferous–Permian mixed siliciclastic, carbonate and evaporite, and spiculitic sediments that developed during multiple phases of extension. The majority of the Mesozoic succession is composed of siliciclastic deposits formed in sag basins and continental platforms. Episodes of Late Jurassic and Early Cretaceous contraction are evident in the eastern part of the archipelago and in nearby offshore areas. Differential uplift related to the opening of the Amerasian Basin and the Cretaceous emplacement of the High Arctic Large Igneous Province created a major hiatus spanning from the Late Cretaceous and early Danian throughout the Svalbard CTSE. The West Spitsbergen Fold and Thrust Belt and the associated foreland basin in central Spitsbergen (Central Tertiary Basin) formed as a response to the Eurekan Orogeny and the progressive northward opening of the North Atlantic during the Paleogene. This event was followed by the formation of yet another major hiatus spanning the Oligocene–Pliocene. Multiple reservoir and source-rock units exposed in Svalbard provide analogues to the prolific offshore acreages in the SW Barents Sea, and are important for the de-risking of plays and prospects. However, the archipelago itself is regarded as a high-risk acreage for petroleum exploration. This is due to Paleogene contraction and late Neogene uplift of the western and central parts in particular. There is an absence of mature source rocks in the east, and the entire region is subjected to strict environmental protection.

Supplementary material: Supplementary material 1–5 containing photographs and descriptions of tectono-stratigraphic elements 1–7 are available at https://doi.org/10.6084/m9.figshare.c.6404502.

Located at the northwestern corner of the Eurasian continental plate (Enclosure D), the Norwegian High-Arctic Svalbard archipelago represents an uplifted and exposed part of the western Barents Shelf (Fig. 1). Because of its position, the archipelago offers insights into the structural evolution of the western Barents Shelf margin and adjacent Arctic regions, such as NE Greenland. In particular, the rocks in Svalbard record the events related to the opening of the NE Atlantic and Arctic oceans. The Carboniferous–Paleogene sedimentary succession provides analogues to the age-equivalent strata in the basins offshore. Geological and geophysical data from the archipelago are frequently used in regional resource estimates and to de-risk prospects on the Barents Shelf. Despite the many similarities, especially in the Upper Paleozoic–Mesozoic platform successions, the structural evolution of Svalbard differs from the oil- and gas-bearing offshore basins by the absence of extensional tectonics related to the development of the Late Jurassic North Atlantic rift system and the presence of thrust tectonics related to the Eurekan Orogeny.

Industrial commercial petroleum exploration in Norway started in Svalbard in the early 1960s, before the first North Sea concession round in 1965. No commercial discoveries were made on the archipelago (Senger *et al.* 2019) – which is arguably positive in hindsight, given the unique and fragile ecosystem of Svalbard. Nonetheless, Svalbard's outcrops have been instrumental in training petroleum geologists from Norway and elsewhere to decipher petroleum system elements better and in improving understanding of other parts of the Norwegian Continental Shelf.

In the Svalbard Composite Tectono-Sedimentary Element (SCTSE), as in the southwestern Barents Sea (SWBS), deep burial, probably at its maximum during the late Paleogene, followed by severe uplift during the late Neogene (Nyland *et al.* 1992; Dimakis *et al.* 1998; Lasabuda *et al.* 2018, 2021) in combination with Pleistocene glaciations are probably the biggest risk for commercial oil and gas accumulations. Svalbard itself is an extremely high-risk exploration area for oil and gas.

In contrast to the unsuccessful oil exploration, coal mining has been the most important industrial activity in Svalbard for more than a century. Predominantly Russian and Norwegian companies have been mining Paleogene and Carboniferous coal, with *c.* 78 Mt (million metric tons) of Paleocene and *c.* 9 Mt of Mississippian coal having been produced in the archipelago since the beginning of industrial mining (Jochmann *et al.* 2015). Today, there is one active coal mine in Barentsburg and one in Longyearbyen, where Paleocene, high-volatile, bituminous coal is extracted.

In this chapter, we present a comprehensive and up-to-date overview of the geology and petroleum geology of the SCTSE, herein defined as the Carboniferous–Paleogene sedimentary rock succession and its associated structural elements. As such, the underlying economic basement consisting of Devonian and older sedimentary rocks, as well

From: Drachev, S. S., Brekke, H., Henriksen, E. and Moore, T. (eds) *Sedimentary Successions of the Arctic Region and their Hydrocarbon Prospectivity*. Geological Society, London, Memoirs, **57**,
https://doi.org/10.1144/M57-2021-36

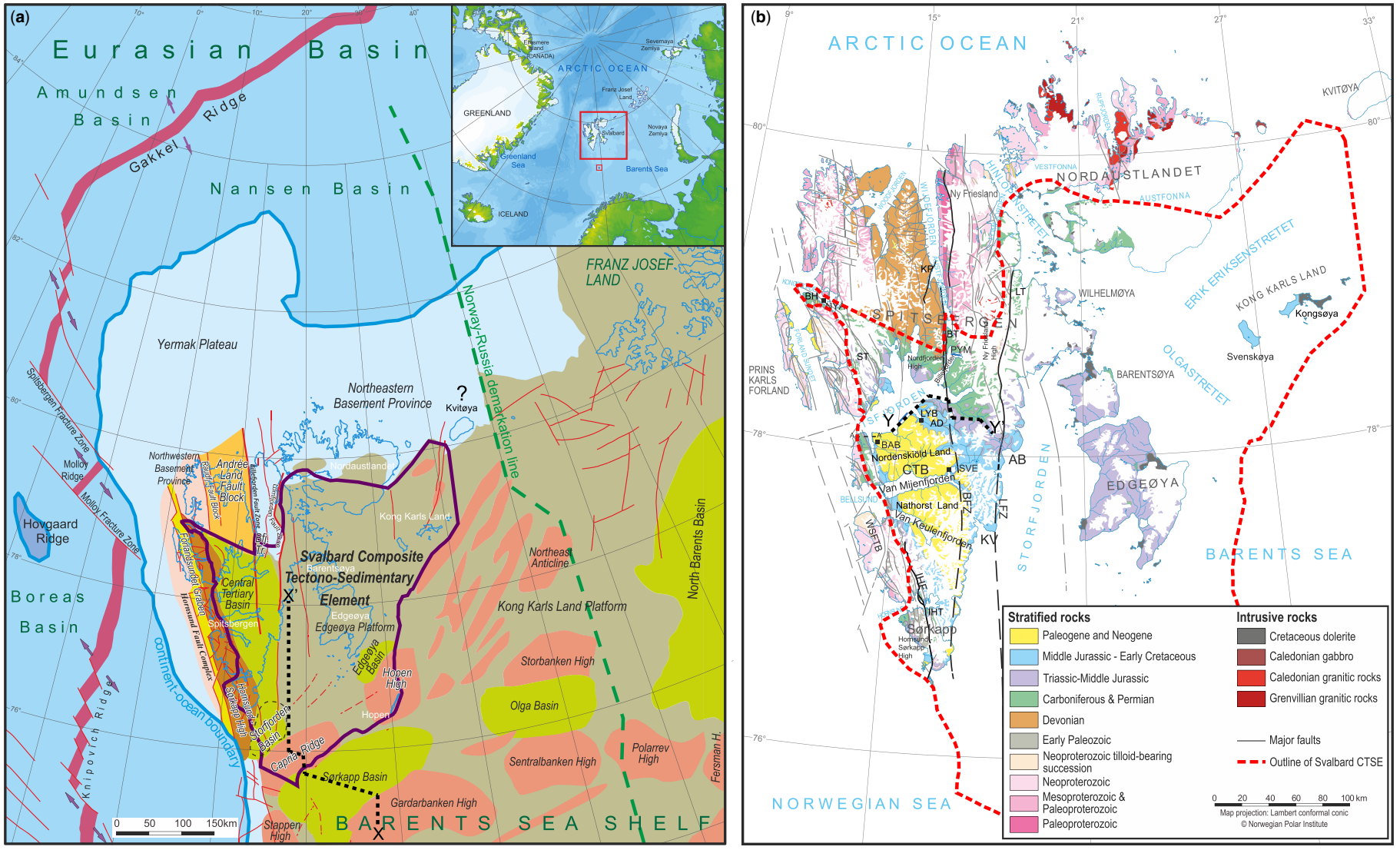

Fig. 1. (**a**) Structural framework of the Svalbard Composite Tectono-Sedimentary Element. (**b**) Geological map of Svalbard excluding Bjørnøya. Only the area within the black line in (a) and stippled line in (b) is discussed in this paper. AB, Agardhbukta; BAB, Barentsburg; KV, Kvalvågen; LYB, Longyearbyen; NYÅ, Ny Ålesund; PYM, Pyramiden; SVE, Svea. Source: geological maps from Dallmann (2015) and the Norwegian Polar Institute.

as Precambrian igneous and metamorphic rocks, are not considered. The SCTSE (Fig. 1a, b) is located between approximately 76° and 80° N and 12° and 30° E, and covers an area of c. 121 000 km^2. The offshore areas adjacent to the SCTSE (Enclosure E) are presented in the North Barents CTSE chapter (Lundschien *et al*. 2023) while the western margin, including the WSFTB, is discussed in the West Barents Sheared Margin CTSE chapter (Faleide *et al*. in review).

Age

The Carboniferous–Lower Cretaceous succession is stratigraphically almost complete, whereas the younger succession is stratigraphically less complete with a major regional hiatus spanning the latest middle Albian–latest Danian (Steel and Worsley 1984; Jochmann *et al.* 2020). Although not substantiated by any biostratigraphic data, a possible Oligocene age has previously been suggested for the youngest part of the Paleogene succession of the Central Tertiary Basin (CTB). In addition, a sliver of middle Oligocene marine mudstone occurs in a fault-bound basin within the West Spitsbergen Fold and Thrust Belt (WSFTB: Schaaf *et al.* 2021).

Geographical location and dimensions

The Svalbard archipelago, which includes all islands between 71°–81° N and 10°–35° E, is bounded in the west and north by Cenozoic passive continental margins facing the NE Atlantic and Arctic oceans, respectively (Fig. 1a; Enclosure A) (Faleide *et al.* 2008; Piepjohn *et al.* 2016). Nearly 60% of the exposed landmasses of the Svalbard archipelago is covered by glaciers (slightly less extensive glacier cover within the SCTSE). The basement provinces and WSFTB in Svalbard are characterized by an alpine topography with rugged peaks ranging up to 1700 m above sea level, whereas the landscape within the SCTSE is dominated by lower and less alpine 'table-top' mountains reflecting the presence of layered sedimentary strata. The sparse high-Arctic vegetation in combination with current retreating glaciers enable detailed outcrop investigations. The nearby offshore areas are generally very shallow (typically 50–150 m water depths), whereas most of the larger fjords tend to be deeper, recording a significant deepening in their outer parts (e.g. outer Isfjorden: >400 m deep).

Principal datasets

The principal datasets used and reviewed in this paper include large amounts of conventional outcrop data (i.e. sedimentological, stratigraphical and structural data) derived from published papers and recent unpublished studies, well data including core and wireline logs, onshore and offshore 2D reflection seismic, and potential field data (magnetic and gravimetric data). The locations of wells and seismic lines are shown in Figure 2.

Wells

This study utilizes available data from 18 petroleum exploration wells drilled in Svalbard from 1961 to 1994 (Table 1) (Nøttvedt *et al.* 1993; Senger *et al.* 2019), research boreholes in Adventdalen (DH1–DH8: Olaussen *et al.* 2019) and Nathorst Land (well BH 10-2008 'Sysselmannbreen': Johansen *et al.* 2011; Johannessen *et al.* 2011), and selected coal exploration boreholes drilled by the Norwegian coal mining company Store Norske Spitsbergen Kullkompani (SNSK).

Seismic data

Figure 2 shows the 2D reflection seismic data coverage, both onshore and offshore. Seismic imaging and resolution, as exemplified in Figure 3, are major problems offshore the western part of the SCTSE due to high velocities (> 4–5 km s^{-1}) in strongly lithified sediments on the seafloor (Eiken 1985, 1994).

Onshore, problems arise from the heterogeneous permafrost (Johansen *et al.* 2003). Seismic profiles are confined to the main fjords, and the onshore seismic data are restricted to the main valleys of Nordenskiöld Land (Bælum and Braathen 2012; Braathen *et al.* 2012) and Nathorst Land (Johansen *et al.* 2011). Seismic data have been presented by Eiken (1994), Bergh *et al.* (1997), Grogan *et al.* (1999, 2000), Johannessen

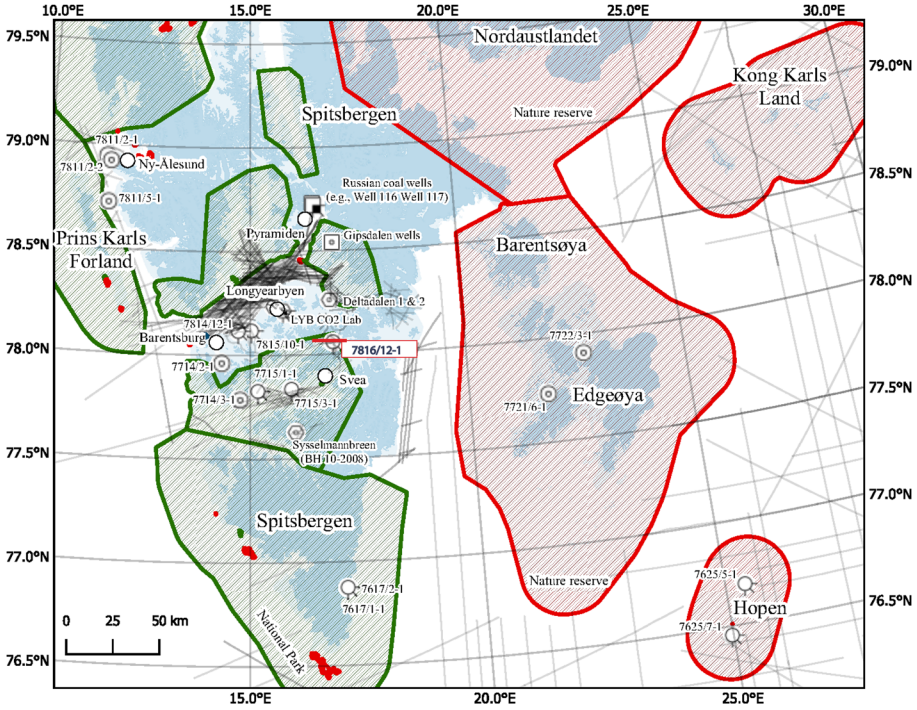

Fig. 2. Principal datasets. 2D conventional seismic lines are shown as grey lines. Hydrocarbon exploration wells are marked with numbers 7*nnn*/*n*-*n* and follow the annotation recommended by the Norwegian Petroleum Directorate (NPD). Others are coal drilling or R&D wells. The red line at 7816/12-1 is the location of the seismic cross-section in Figure 8. The green hachured areas are national parks, while red hachured areas are national reserves.

Table 1. *Exploration boreholes from 1961 to the last exploration, which was well drilled in 1994*

No.	NPD well ID Borehole name	Easting Northing	Longitude Latitude	Spudded Completed	Operating company	Elevation KB (m) Total depth (m MD)	Youngest age Youngest formation	Oldest age Oldest formation	Likely reservoir target Tectono-stratigraphic element (TSE)	Likely reason for drilling and other comments
0	-	422970	11°23'23"	summer 1961	NPN	0	Early Permian	Pre-Devonian		Surface mapping with some oil stains from airport planning. Easily accessible coastal area.
	Kvadehuken I	8766727	78°57'03"	6/16/1963		479	Gipshuken Fm	Hecla Hoek	TSE 3	
1	*7714/2-1*	484198	14°20'36"	6/9/1963	NPN	7.5	Early Cretaceous	Late Triassic	Wilhelmøya Subgroup	Surface mapping. Structurally complex area in WSFB.
	Grønnfjorden I	8654805	77°57'34"	8/12/1967		971.6	Carolinefjellet Fm	De Geerdalen Fm	TSE 4	
2	*7715/3-1*	522340	15°58'00"	8/1/1965	Amoseas	18	Paleocene	Early Permian	Numerous potential reservoirs	Surface mapping, but drilled on an offset structure as confirmed by later 2D seismic acquisition. First true deep wildcat.
	Ishøgda I*	8640201	77°50'22"	3/15/1966		3304	Grumantbyen Fm	Gipshuken Fm	TSE 3, TSE 4	
3	*7714/3-1*	493959	14°46'00"	8/23/1967	NPN	0	Late Jurassic	?	Wilhelmøya Subgroup?	Surface mapping and some gas seepage onshore. Easily accessible coastal area.
	Bellsund I	8634503	77°47'00"	8/10/1981		405	Agardhfjellet Fm	?	TSE 4	
4	*7625/7-1*	761068	25°01'45"	8/11/1971	Fina	9.1	Late Triassic	Middle Triassic	?	Surface mapping.
	Hopen I*	8507624	76°26'55"	9/29/1971		908	De Geerdalen Fm	Botneheia Fm	TSE 4	
5	*7722/3-1*	678904	22°41'50"	4/2/1972	CFP	84	Late Permian	Ordovician	?	Surface mapping. Regional geophysical data.
	Raddedalen	8660316	77°54'10"	7/12/1972		2823	Kapp Starostin Fm	Horbyebreen Fm	TSE 1, TSE 3	
6	*7721/6-1*	659992	21°50'00"	6/29/1972	Fina	144.6	Middle Triassic	Pre-Devonian	?	Surface mapping. Regional geophysical data.
	Plurdalen	8638282	77°44'33"	10/12/1972		2351	Botneheia Fm	?	TSE 0, TSE 1, TSE 3	
7	*7811/2-1*	422970	11°23'23"	9/1/1972	NPN	0	Early Permian	Pre-Devonian	?	Surface mapping.
	Kvadehuken II	8766727	78°57'03"	6/19/1973		479	Gipshuken Fm	Hecla Hoek	TSE 0, TSE 3	
8	*7625/5-1*	767641	25°28'00"	6/20/1973	Fina	314.7	Late Triassic-Middle Jurassic	Middle Carboniferous	Numerous potential reservoirs	Some limited offset 2D seismic offshore Hopen. Otherwise surface mapping.
	Hopen II*	8535807	76°41'15"	10/20/1973		2840	Wilhelmøya Subgroup	Ebbadalen Fm	TSE 2, TSE 3, TSE 4	
9	*7811/2-2*	424853	11°33'11"	8/13/1973	NPN	0	Early Permian	?	?	Surface mapping.
	Kvadehuken III	8764140	78°55'32"	6/16/1974		394	Gipshuken Fm	?	TSE 0, TSE 3	
10	*7811/5-1*	422845	11°28'40"	8/15/1974	NPN	5	Oligocene	Pre-Devonian	?	Surface mapping. Easy access to drill site
	Sarstangen‡	8741814	78°43'36"	12/1/1974		1113	Sarstangen conglomerate	Hecla Hoek	TSE 6	
11	*7815/10-1*	500325	15°02'00"	11/13/1974	TA	12	Paleocene	Early Permian	Numerous potential reservoirs	Surface mapping. Easy access to drill site and logistics, at a Russian coal mining settlement.
	Colesbukta‡	8671916	78°07'00"	12/1/1975		3180	Basilika Fm	Gipshuken Fm	TSE 3, TSE 4	
12	*7617/1-1*	552582	17°05'30"	9/11/1976	NPN	6.7	Early Cretaceous	Late Triassic-Middle Jurassic	Wilhelmøya Subgroup	Surface mapping.
	Tromsøbreen I	8533670	76°52'31"	9/19/1977		990	Carolinefjellet Fm	Wilhelmøya Subgroup	TSE 4	
13	*7715/1-1*	503990	15°11'15"	1/10/1985	TA	15.13	Eocene	Carboniferous (?)	Numerous potential reservoirs	Surface mapping.
	Vassdalen II‡	8639407	77°49'57"	7/14/1987		2481	Frysjaodden Fm	Billefjorden Gp (?)	TSE 1 (?), TSE 3, TSE 4	
14	*7617/1-2*	552650	17°05'38"	7/20/1987	T-PG	6.7	Early Cretaceous	Early Permian	Numerous potential reservoirs	Surface mapping.
	Tromsøbreen II‡	8533700	76°52'31"	8/24/1988		2337	Carolinefjellet Fm	Gipshuken Fm	TSE 2, TSE 3, TSE 4	
15	*7715/1-2*	503990	15°11'15"	2/28/1988	TA	15.13	Eocene	Middle Triassic	Numerous potential reservoirs	Surface mapping.
	Vassdalen III‡	8639407	77°49'57"	9/1/1989		2352	Frysjaodden Fm	Botneheia Fm	TSE 3, TSE 4	
16	*7816/12-1*	544775	16°56'31"	1/17/1991	NH/SNSK	182.5	Early Cretaceous	Middle Carboniferous	Numerous potential reservoirs	Sparse 2D seismic acquisition prior to drilling. Comprehensive surface mapping.
	Reindalspasset I*	8665611	78°03'28"	4/11/1991		2315	Carolinefjellet Fm	Hultberget Fm	TSE 1, TSE 3, TSE 4	
17	*7814/12-1*	493560	14°53'38"	2/22/1994	SNSK/TA/NH	5	Paleocene	Early Cretaceous	Helvetiafjellet Formation	Surface mapping. Nearby coal exploration.
	Kapp Laila I*	8671260	78°06'52"	5/8/1994		503.5	Basilika Fm	Carolinefjellet Fm	TSE 4	

*wells with reported gas shows

‡wells that tested gas in producible quantities

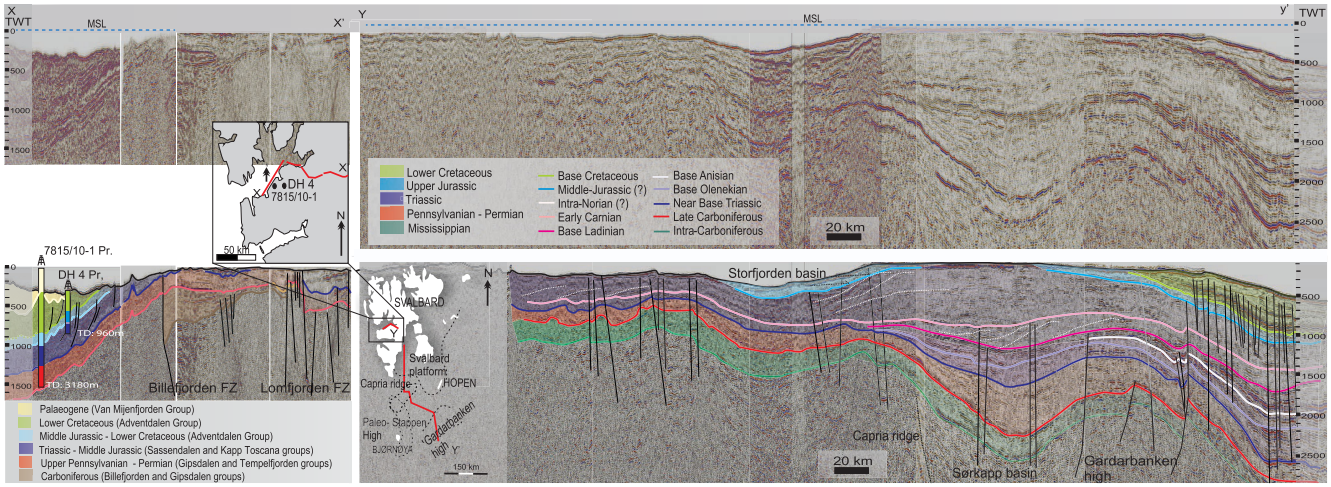

Fig. 3. Uninterpreted and interpreted composite seismic lines crossing central Spitsbergen from west to east, continuing offshore in a southwards direction to the Garderbanken High south of the SCTSE. The location of line X–X′ is shown in Figure 1a and the location of Y–Y′ is shown in Figure 1b. MSL, mean sea level; Pr., well projected; TD, total depth; TWT, two-way travel time.

et al. (2011), Blinova *et al.* (2013), Senger *et al.* (2013), Anell *et al.* (2014*a*, *b*, *c*) and Roy *et al.* (2015).

Six of the exploration wells (Reindalspasset, Colesbukta, Kapp Laila, Vassdalen II and III, and Ishøgda) and two research boreholes (Sysselmannbreen DH 2 and DH4) can be tied to 2D seismic data (Fig. 3). Only the prospect in the Reindalspasset well 7816/12-1 was drilled based on sparse 2D acquisition and limited seismic mapping, and tested a conventional play model (Senger *et al.* 2019).

Outcrop and subsurface studies

There has been a long history of geological investigations in Svalbard, with much of the early work focusing particularly on lithological and structural mapping, palaeontology, and various stratigraphic aspects of the sedimentary rock succession. This work has been summarized by a series of geological maps published by the Norwegian Polar Institute (NPI) and in numerous articles and books (e.g. Steel and Worsley 1984; Harland 1997; Dallmann *et al.* 1999; Vigran *et al.* 2014; Dallmann 2015). Digital outcrop models, particularly from drone-based acquisition, are increasingly available and shared via the Svalbox repository (Senger *et al.* 2021). The efforts of previous investigations thus form the framework for this paper.

Gravity and magnetic data were acquired and compiled by the Geological Survey of Norway and are presented in Nasuti *et al.* (2015). The regional aeromagnetic data were acquired with relatively large line spacing (2–8 km) and high sensor elevation (250–1550 m), and are supplemented by ship-based magnetic data in Isfjorden (Senger *et al.* 2013). Gravity data incorporate both relatively dense surface stations, especially along the coastlines, and marine surveys around Svalbard.

Regional magnetotelluric (MT) profiles were acquired to characterize the geothermal potential of Nordenskiöld Land (Beka *et al.* 2016, 2017*b*) and Brøggerhalvøya (Beka *et al.* 2017*a*), and provide additional constraints on the regional tectonic structure of the area through subsurface conductivity profiles.

Tectonic setting, boundaries and main tectonic/erosional/depositional phases

The Latest Devonian Cenozoic evolution of the SCTSE is grouped into seven separate tectono-sedimentary elements (TSE 1–TSE 7). The main tectonic events, lithostratigraphic subdivision of the investigated succession and the hydrocarbon play elements are summarized in Figure 4.

The western boundary of the SCTSE is bounded along the eastern margin of the highly deformed WSFTB, which locally includes overthrusted Precambrian–Paleogene successions. The inverted Carboniferous Capria Ridge and southern rim of the Hopen High (Anell *et al.* 2016) mark the southern edge of the SCTSE (Fig. 1a). The Carboniferous and part of the Permian are mainly fault bounded to basement in the north and NE, which defines the northern boundary of the SCTSE. Elsewhere, the northern boundary is defined by the last cropping out Carboniferous–Paleogene strata overlying the economic basement. Initial subsidence during the earliest Mississippian, locally late Fammenian, promoted the development of an interior continental basin within a continental platform (TSE 1). The basin fill is assigned to the Billefjorden Group. The development during this phase is partly disputed, with the discussion evolving around a pre- or synkinematic structural regime. Extensional basins are suggested in the southern and western parts of Spitsbergen (Cutbill and Challinor 1965; Holliday and Cutbill 1972; Gjelberg and Steel 1981; Braathen *et al.* 2011; Maher and Braathen 2011; Smyrak-Sikora *et al.* 2021).

The Late Mississippian–Middle Pennsylvanian rifting resulted in the formation of a series of elongated, north–south-orientated fault-bounded basins on Spitsbergen (McCann and Dallmann 1996; Braathen *et al.* 2011; Maher and Braathen 2011; Bælum and Braathen 2012; Smyrak-Sikora *et al.* 2019, 2021). This synrift tectono-sedimentary element (TSE 2) is well documented in the Billefjorden Trough of central Spitsbergen (Fig. 1b).

Waning fault activity and regional subsidence during the Late Pennsylvanian–Early Permian in combination with continued northward continental drift promoted the development of an extensive and long-lived carbonate platform (TSE 3: Fig. 4) (Stemmerik and Worsley 2005). This post-rift TSE 3 comprises the upper part of the Gipsdalen Group (Fig. 4).

Renewed extension in the late Early Permian (Artinskian) is linked to the Permian–Triassic development of the North Atlantic rift system along the western margin of the Barents Sea and East Greenland (Seidler *et al.* 2004; Riis *et al.* 2008; Clark *et al.* 2014; Anell *et al.* 2016; Tsikalas *et al.* 2021). A cool-water carbonate platform developed during this synrift phase (TSE 4: Fig. 4). Fault-related uplift of the basin margins controlled the facies and thickness variations of the spiculite, carbonate and siliciclastic facies in the Tempelfjorden Group.

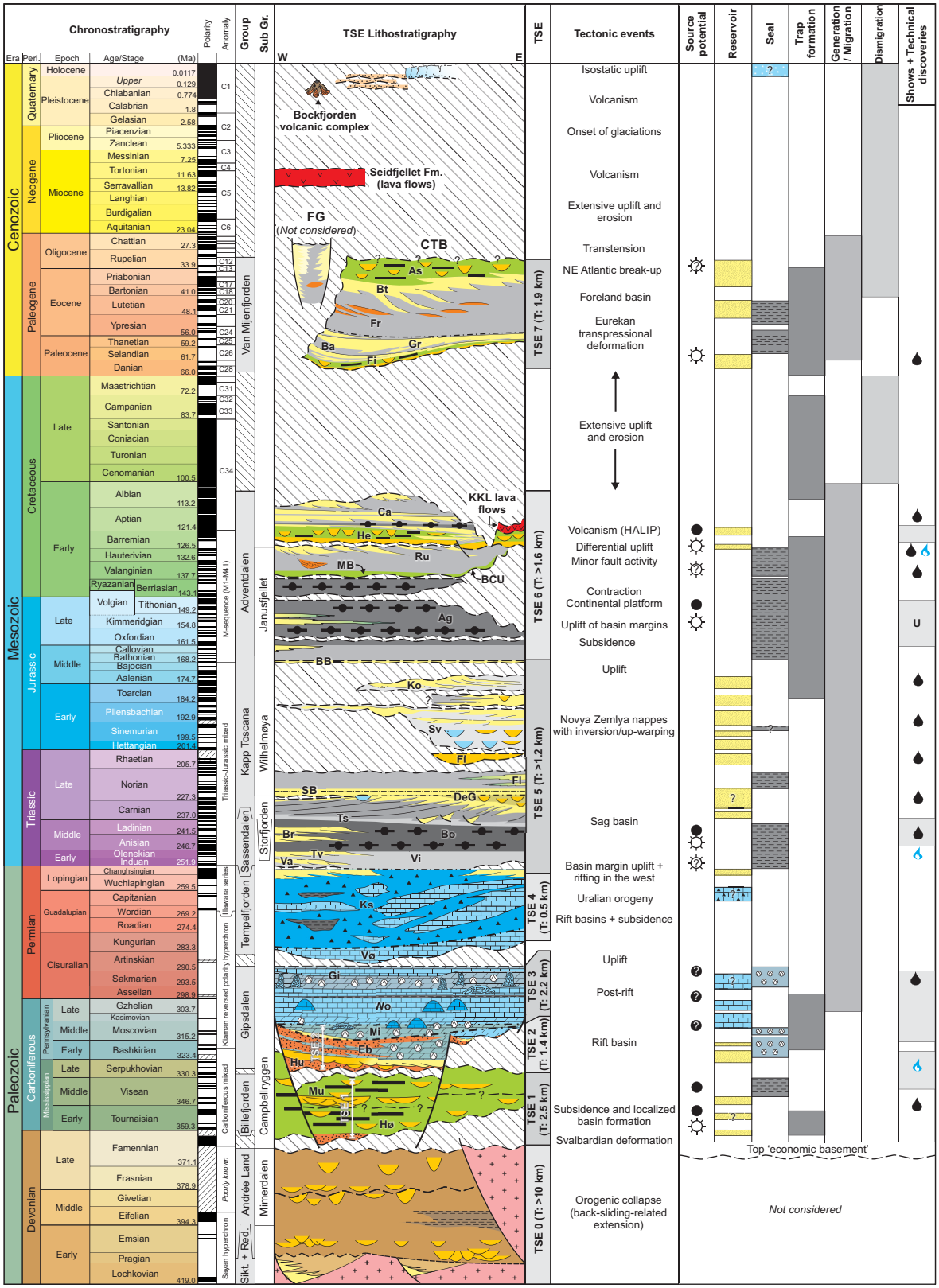

Fig. 4. Composite summary of chronostratigraphy/lithostratigraphy, tectonic events and petroleum systems (i.e. previous petroleum systems) of the tectono-sedimentary sequences (TSE 1–TSE 6) documented in this study. The geological timescale is after Gradstein and Ogg (2020: https://timescalefoundation.org). The column is based on the most recent stratigraphic work available, including that of Vigran *et al.* (2014), Paterson *et al.* (2016), Smelror *et al.* (2018), Koevoets *et al.* (2018), Jochmann *et al.* (2020) and Śliwińska *et al.* (2020). BCU, Base Cretaceous Unconformity. Abbreviations of lithostratigraphic units and structural elements (from top down): Ag, Agardhfjellet Fm; As, Aspelintoppen Fm; Ba, Battfjellet Fm; BB, Brentskardhaugen Bed; Bo, Botneheia Fm; Br, Bravaisberget Fm; Bt, Battfjellet Fm; Ca, Carolinefjellet Fm; CTB, Central Tertiary Basin; DeG, De Geerdalen Fm; Eb, Ebbadalen Fm; FG, Forlandsundet Graben; Fi, Firkanten Fm; Fl, Flatsalen Fm; Fr, Frysjaodden Fm; Gi, Gipshuken Fm; Gr, Grumantbyen Fm; He, Helvetiafjellet Fm; Hø, Hørbybreen Fm; Hu, Hultberget; KKL lava flows, Kong Karls Land lava flows; Ko, Kongsøya Fm; Ks, Kapp Starostin Fm; MB, Myklegardfjellet Bed; Mi, Minkenfjellet Fm; Mu, Mumien Fm; Ru, Rurikfjellet Fm; SB, Slottet Bed; Sv, Svenskøya Fm; Ts, Tschermakfjellet Fm; Tv, Tvillingodden Fm; Va, Vardebukta Fm; Vi, Vikinghøgda Fm; Vø, Vøringen Member; Wo, Wordiekammen Fm.

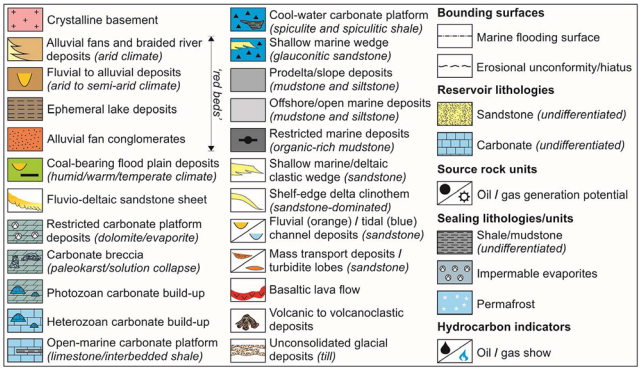

Fig. 4. *Continued.*

Early Triassic–Middle Jurassic regional subsidence resulted in the development of a sag basin dominated by siliciclastic deposition (TSE 5: Fig. 4). The Middle Triassic–Upper Triassic NW-prograding delta sourced from the denudation from the Uralide mountains and Fennoscandian Shield reach Spitsbergen in the Carnian (Anell *et al.* 2014*a*; Klausen *et al.* 2019). In addition, a less prominent western source contributed to deposition in the western and southern parts of the SCTSE (Mørk *et al.* 1982; Krajewski and Weitschat 2015; Czarniecka *et al.* 2020). A condensed Norian–Pliensbachian succession, <10 m thick and with numerous internal hiatuses in the west, thickens eastwards to a >200 m-thick, stratigraphically almost complete, succession (Fig. 4). The subsidence of the succession in the east is suggested to be linked to the Novaya Zemlya Orogen. (Olaussen *et al.* 2018; Müller *et al.* 2019).

Late Middle Jurassic–Early Cretaceous regional subsidence with uplift in the north and NW formed a continental, siliciclastic platform (TSE 6: Fig. 4). Early Cretaceous circum-Arctic magmatism resulted in the emplacement of the High Arctic Large Igneous province (HALIP), which eventually became a prominent sediment source from the Barremian onwards (Maher 2001; Grantz *et al.* 2011; Polteau *et al.* 2016). Local extensional faulting occurred on Spitsbergen (Onderdonk and Midtkandal 2010) and some minor contraction took place in the east, at Kong Karls Land and Kong Karls Land Platform (Grogan *et al.* 1999, 2000; Olaussen *et al.* 2018).

The latest middle Albian–latest Danian hiatus records exhumation of the entire SCTSE with a significant component of northerly uplift, probably induced by magmatism and the opening of the Amerasian Basin north of Svalbard (Maher 2001). Plate tectonic reorganization initiated by the opening of the North Atlantic Ocean may also have contributed to the uplift and the development of this major hiatus (e.g. Faleide *et al.* 2008). The occurrence of Late Cretaceous terrestrial and marine microfloras in Paleocene strata in southern Spitsbergen indicates erosion and reworking of previous deposited Upper Cretaceous strata (Smelror and Larssen 2016).

North-directed opening of the North Atlantic Ocean culminated with the formation of a transform fault along the De Geer Zone, linking the Atlantic and Arctic basins. This zone had a major impact on the Paleogene development of the SCTSE. During the Paleocene, dextral movement between the Eurasian and Greenland plates caused transpression-induced crustal shortening (e.g. Bergh *et al.* 1997; Leever *et al.* 2011), with the formation of the WSFTB and its flanking foreland basin, the CTB (Steel *et al.* 1981; Helland-Hansen 1990; Braathen *et al.* 1999; Helland-Hansen and Grundvåg 2020). The foreland basin fill is assigned to TSE 7 (Fig. 4) and further suggests that the main phase of contraction-driven uplift in the west, along the De Geer Zone, appeared in the Eocene (TSE 7: Fig. 4). Subsequent graben formation within the De Geer Zone and WSFTB during the late Eocene–Oligocene indicates a shift from transpression to transtension driven by changes in plate motion (Maher *et al.* 1997, 2020; Braathen *et al.* 1999).

Finally, the current Neogene passive-margin development was accompanied by recurrent periods of uplift, erosion and glaciation from 3.6 Ma (Knies *et al.* 2009). Crustal thinning and the onset of oceanic spreading close to western Spitsbergen probably governed the development of a Neogene hiatus across the Svalbard archipelago and the surrounding shelf areas (Green and Duddy 2010).

The central and western parts of the archipelago and the northwestern part of the Barents shelf margin in particular have been subjected to significant uplift over the last few million years (Dimakis *et al.* 1998; Henriksen *et al.* 2011*a*; Lasabuda *et al.* 2018), and the presence of thick pre-glacial (probably Miocene and Pliocene) and glacial (late Pliocene and Pleistocene) clastic wedges offshore west Spitsbergen (Hjelstuen *et al.* 1996) suggests a net denudation of *c.* 3 km (Riis and Fjeldskaar 1992). This is in overall agreement with uplift estimates in the range 2.5–3.5 km based on organic geochemical studies (Throndsen 1982; Marshall *et al.* 2015; Olaussen *et al.* 2019). However, the westernmost margin of the SCTSE might have been subjected to a higher magnitude of uplift or a higher temperature gradient. Remnants of Pleistocene glacial deposits occur locally onshore Spitsbergen, indicating multiple glaciations (Ingólfsson and Landvik 2013). Uplift of 9 mm a^{-1} is ongoing at present in central western Spitsbergen. However, only 1 mm a^{-1} of this is attributed to isostatic rebound due to deglaciation following the Late Weichselian glaciation (Kierulf *et al.* 2022). TSEs 1–7 are summarized below (see Supplementary material 1–7 for outcrop examples):

(1) Uppermost Devonian to Lower Mississippian TSE 1 deposited in an interior continental sag basin possibly related to initial rift stage in SW;
(2) Serpukhovian to Moscovian synrift TSE 2;
(3) Upper Pennsylvanian to Lower Permian – postrift sag/platform TSE 3;
(4) Lower Permian (Artinskian) to the base Triassic synrift TSE 4;
(5) Base Triassic to lower Middle Jurassic – sag basin TSE 5;
(6) Upper Middle Jurassic to Lower Cretaceous – continental platform TSE 6;
(7) Paleogene – foreland basin TSE 7.

Underlying and overlying rock assemblages

Age of underlying basement (consolidated crust) or youngest sedimentary unit

The oldest crystalline basement rocks in Svalbard are dated to 2709 ± 28 Ma (U–Pb zircon ion microprobe: Hellman *et al.* 2001). The youngest rocks below the SCTSE are the metasediments of Middle Fammenian age. Tournaisian–Visean strata exhibit a metasedimentary character in the WSFTB.

Some exploration wells were drilled into metamorphic rocks of Caledonian age (Senger *et al.* 2019) and on Edgeøya an exploration well drilled into carbonate beds of disputed age, possibly being of either Late Devonian or Silurian–Ordovician age at a total drilling depth (TD) of 2283 m (cf. Harland and Kelly 1997). Based on the relatively poor quality of reflection seismic imaging of deeper strata, we suggest that the economic basement in the nearby offshore areas is most likely to be similar to that proven in the onshore areas (Faleide *et al.* 2017).

Age of oldest overlying sedimentary units

The oldest overlying sediments are late Pliocene glacial deposits.

Subdivision and internal structure

One of the main structural characteristics of the SCTSE is the north–south-trending Pennsylvanian rift basins situated along prominent fault zones. In addition, Mesozoic sag basins and platforms, together with the CTB, define the main internal structures of the SCTSE (Fig. 1).

Carboniferous north–south-trending rift basins

The best-exposed example of a north–south rift basin is the Billefjorden Trough between Billefjorden and Austfjorden (Fig. 1b). It is a *c.* 25 km-wide, westward-dipping and southward-plunging half-graben with main the extensional phases occurring during the Serpukhovian–Moscovian (Maher and Braathen 2011; Smyrak-Sikora *et al.* 2019, 2021). The preserved basin fill forms a westward-thickening wedge, up to 2 km thick on the hanging wall of the north–south-striking, eastward-dipping Billefjorden Fault Zone. Reactivation of normal faulting occurred in the Permian and possibly also during the Early Triassic. The southward continuation of the north–south-trending Carboniferous rift basins is documented by exploration well 7816/12-1 (Fig. 2).

Along the northern part of the complex Lomfjorden Fault Zone, a westward-dipping wedge-shaped Lower Carboniferous basin fill occurs in the Lomfjorden Trough (Fig. 1b) (Gjelberg and Steel 1981; Harland 1997; Blomeier *et al.* 2009). The Lomfjorden Trough is bounded to the west by the north–south-striking basement-dominated high: the Ny Friesland High (Figs 1b, 5 & 6). We speculate that the Ny Friesland High is a Carboniferous horst structure and that the Lomfjorden Trough represents the remnants of a larger Carboniferous graben (Fig. 6).

Permian reactivation

Reactivation of the north–south-trending faults was important for later structuring in the SCTSE. Renewed rifting occurred in the late Early Permian. This is particularly evident in southern Spitsbergen, where Upper Permian strata are thin and pinch out across the Sørkapp–Hornsund High. In addition, Artinskian–uppermost Permian deposits appear to be downfaulted (by *c.* 400 m) on the southwestern tip of Sørkapp (Dallmann 2015), thus recording Late Permian fault activity. Thickness variations of the Upper Permian strata demonstrating local fault activity are also observed on the Nordfjorden High (Fig. 6) and Sørkapp–Hornsund High (Hellem 1980; Knag 1980; Blomeier *et al.* 2011; Bond *et al.* 2017) and probably lasted until the early Middle Triassic (Krajewski and Weitschat 2015; Czarniecka *et al.* 2020).

Mesozoic basins and platforms

The Svalbard Platform and the northern part of the Kong Karls Land Platform are the two main internal Mesozoic structures in the SCTSE. Following cessation of Late Paleozoic tectonic activity of the Edgeøya Basin, the Hopen High merged with the Edgeøya Platform to form the Mesozoic Svalbard Platform (Anell *et al.* 2016). Due to poor seismic coverage, its eastern boundary towards the Kong Karls Land Platform is difficult to define. Large, NE-striking Mesozoic synforms and antiforms with Late Mesozoic and Tertiary reverse faults and

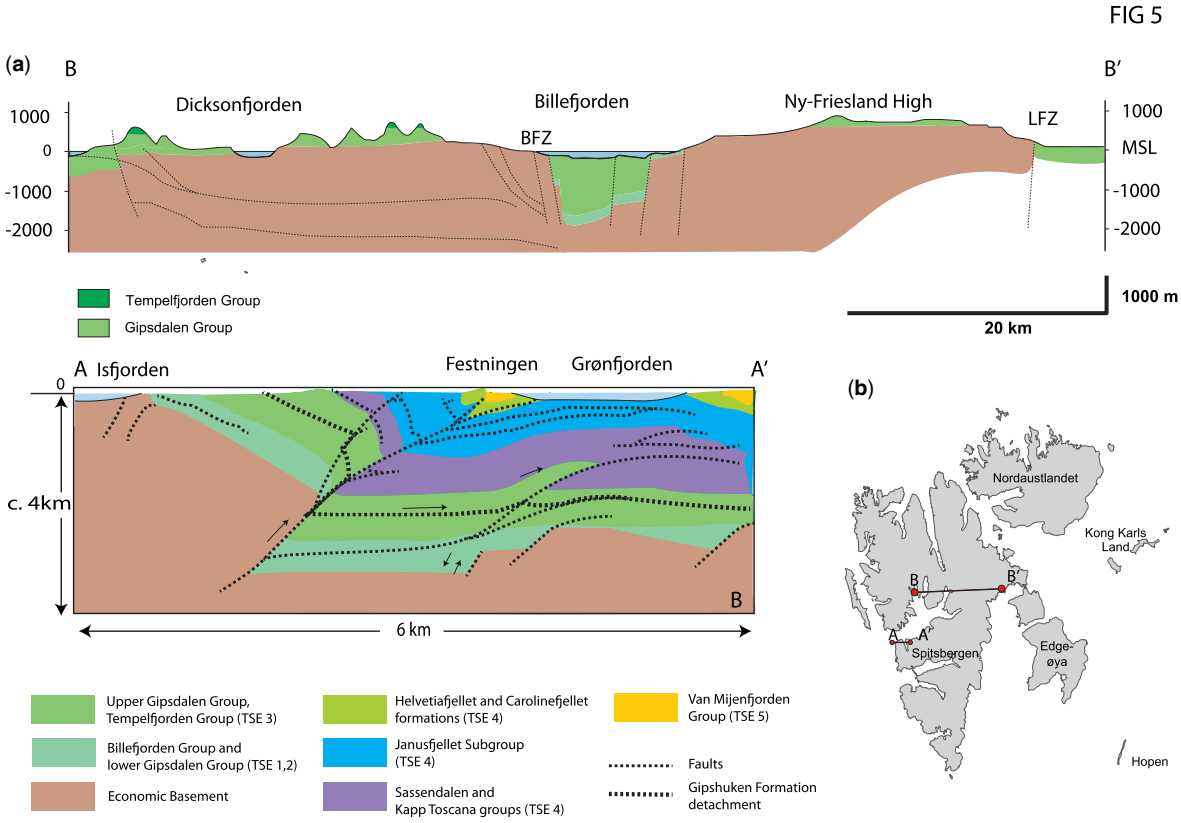

Fig. 5. Cross-sections from Spitsbergen. (**a**) Cross-section from central to eastern Spitsbergen. Lomfjorden Fault Zone from Haremo and Andresen (1992). The locations of the cross-sections are seen in (b). (**b**) Cross-section from the West Spitsbergen Fold and Thrust Belt. The estimated depth of the cross-section is based on poor-resolution offshore seismic data (Bergh *et al.* 1997) and a crude velocity model. Source: (a) modified from Dallmann (2015) and Smyrak-Sikora *et al.* (2019); (b) simplified and modified after Braathen *et al.* (1995).

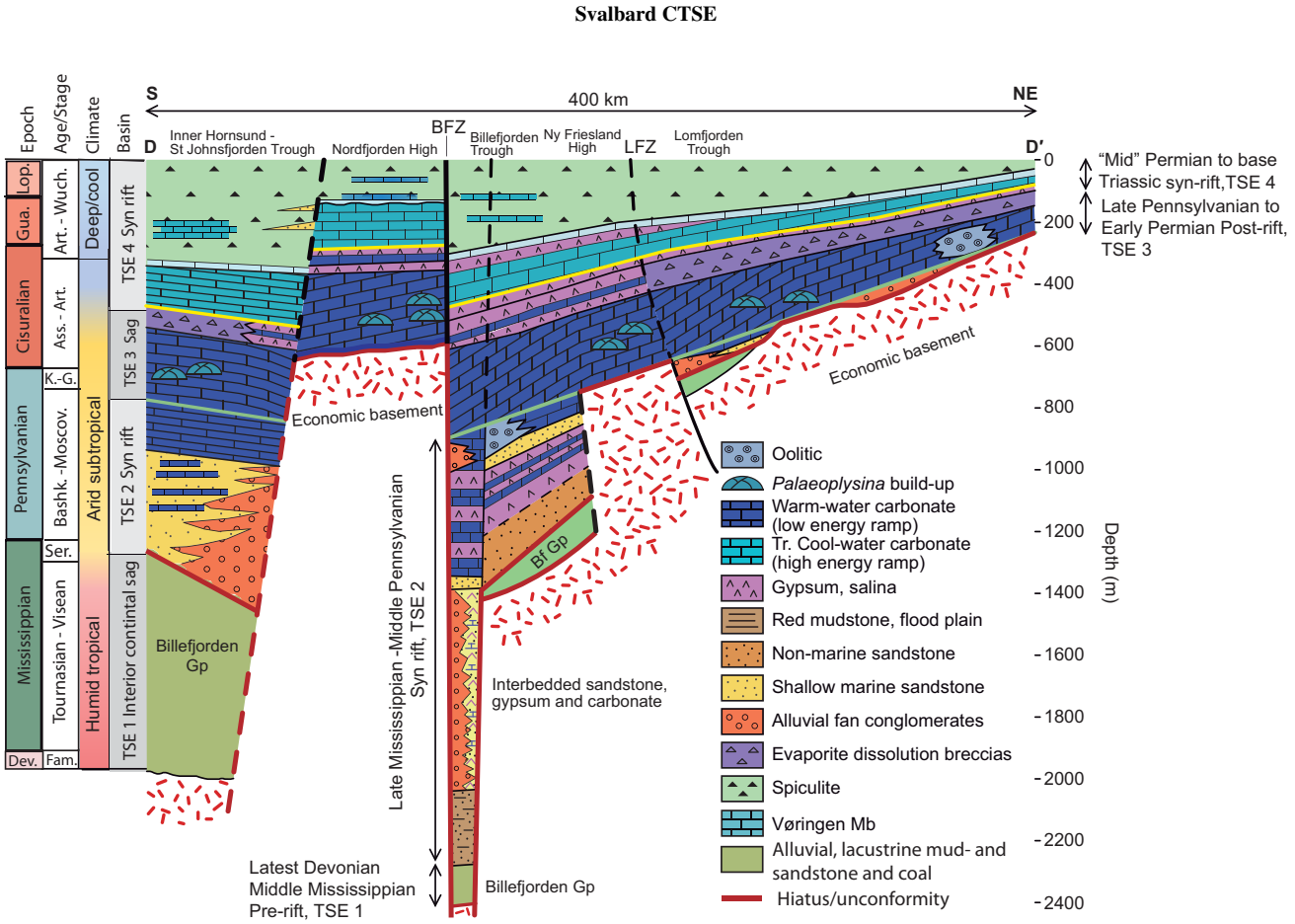

Fig. 6. Stratigraphic structural cross-section of the Carboniferous and Permian from the NE to the southern part of the archipelago. Section from Nordaustlandet, crossing towards the Billefjorden Fault Zone and the Nordfjord High in the SW, and finally southwards to Hornsund (Fig. 1b). Flattened at near top Permian. BFZ, Billefjorden Fault Zone; LFZ, Lomfjorden Fault Zone; Tr. Cool water carbonate, transition to cool-water carbonates. Ny Frisland High as a Carboniferous horst is somewhat speculative.

Lower Cretaceous intrusive or extrusive volcanic rocks characterize the Kong Karls Land Platform (Grogan *et al.* 1999), and gently folded strata with lower Cretaceous volcanic rocks are seen onshore Kong Karls Land (Grogan *et al.* 2000). Two periods of Mesozoic contraction are suggested on Kong Karls Land: one event in the Late Jurassic, probably Kimmeridgian or early Volgian, followed by rejuvenation in the Barremian–Aptian (Olaussen *et al.* 2018). Small-scale rotated fault blocks in the Barremian strata at Kvalvågen suggest instability caused by short-lived tectonic activity along the Lomfjorden Fault Zone.

Reverse faults cutting Permian and the Mesozoic strata are well documented in the Billefjorden Fault Zone at the outer tip of Billefjorden and south of Isfjorden. Haremo and Andresen (1992) showed that the Lomfjorden Fault Zone, west of Agardhbukta, was reactivated by Eocene reverse faulting.

Paleogene basin

The CTB forms an elongated NNW–SSE-orientated syncline that covers an area of *c.* 5000 km^2 in southern and central Spitsbergen. Its margins were initially bounded by a series of north–south-orientated faults. Uplifted terranes to the north and east were the main source areas for the Paleocene basin fill (e.g. Steel *et al.* 1981, 1985; Bruhn and Steel 2003; Petersen *et al.* 2016). Structural outliers containing correlative Paleocene strata at Brøggerhalvøya (and elsewhere) may indicate that the Paleocene basin was covering a much larger area than presently preserved (Jochmann *et al.* 2020). During the contraction in Eocene, the WSFTB continued to rise, and flexural loading along the western basin margin thus assisted in maintaining the asymmetrical basin shape, being deepest in the west and shallowing significantly eastwards (Helland-Hansen and Grundvåg 2020). The Paleogene deformed Storfjorden Basin is fault bounded by the Sørkapp–Hornsund High and the anticlinal structure above the Capri Ridge (Anell *et al.* 2016).

The CTB probably developed into a wedge-top basin during the final stages of crustal deformation. The extent of the Eocene basin to the south and east is unknown but it is most likely to have continued far beyond its present-day extent.

After the main transpressional phase in the Eocene, transtensional movements along the Hornsund Fault Zone resulted in the formation of a series of basins along western Spitsbergen, including the Forlandsundet Graben.

Sedimentary fill

Total thickness

The thickness of the Carboniferous–Permian successions (TSE 1–TSE 4: Fig. 4) varies from 380 to 1800 m, whereas the Mesozoic successions (TSE 5–TSE 6: Fig. 4) vary from 1480 to 2370 m, thus adding up to 1860 and 4170 m, respectively. The Paleogene succession (TSE 7: Fig. 4) is only preserved in western and central Spitsbergen (Fig. 1a, b) where it varies from 0 to 1700 m. As such, the total thickness of the SCTSE may reach 5870 m. However, this number is somewhat uncertain due to Paleogene shortening of pre-Paleogene strata, particularly in western Spitsbergen (Braathen *et al.* 1999).

None of the nearby seismic lines that were available for this study has been depth converted due to uncertain interval

velocities, which may cause large uncertainties during attempts to estimate thicknesses.

Lithostratigraphy and depositional systems

TSE 1: Tournaisian–Visean Billefjorden Group. The continental sediments of the Billefjorden Group mark the onset of the Mississippian, locally possiblly late Fammenian, deposition in the SCTSE. The basal surface is a first-order sequence boundary (cf. Embry 2009), recording large-scale tectonic reorganization (i.e. from the Svalbardian deformation to an interior continental basin). In central Spitsbergen, the basal unconformity is overlain by a *c.* 100 m-thick coarse-grained unit of fluvial and lacustrine deposits assigned to the lower part of the Hørbybreen Formation (Fig. 4). In western Spitsbergen, deposition started later with the accumulation of fine-grained floodplain deposits assigned to the Tournaisian Orustdalen Formation. Lopes *et al.* (2018) suggested a late Tournaisian–late Visean hiatus in the Hørbybreen Formation. This coincides with a shift in depositional environments from a coarse-grained sand- and gravel-dominated braidplain to a fine-grained, vegetated floodplain dissected by meandering rivers (e.g. Steel and Gjelberg 1981). In the Billefjorden Trough, coarse-grained braided stream deposits are locally overlain by heterolithic and coal-bearing floodplain fines. This formation thickens northwards along the Billefjorden Fault Zone and pinches out towards the underlying basement in the east. The gradual transition from deposits consistent with wetlands into floodplain red beds with calcrete in the Serpukhovian–Bashkirian Hultberget Formation records a change from humid to semi-arid or arid tropical climate. A more detailed description of TSE 1 is available in Supplementary material 1.

TSE 2: Serpukhovian–Moscovian lower Gipsdalen Group. Deposition of the lower Gipsdalen Group took place in a series of narrow, north–south-elongated rift basins under overall arid to semi-arid climatic conditions. In the Billefjorden Trough, deposition occurred in three distinctive phases. The basal, fluvial-dominated Hultberget Formation and the paralic Ebbaelva Member of the Ebbadalen Formation were deposited during early rifting in an overall symmetrical basin (Johannessen and Steel 1992; Smyrak-Sikora *et al.* 2019). During the main extensional phase and half-graben development, wedge-shaped alluvial fans of the Ebbadalen Formation prograded basinwards from the footwall in the west, interfingering with mixed carbonates, siliciclastics and evaporites in more distal locations to the east. During the late rift and early post-rift stages, shallow-marine siliciclastics and carbonates of the Moscovian Minkinfjellet Formation were deposited along the eastern and western basin margins, whereas interbedded gypsum and carbonate accumulated in the central parts of the basin (Fig. 4) (Smyrak-Sikora *et al.* 2021). Cyclicity and facies changes were due to a combination of tectonically induced subsidence and eustatic sea-level changes governed by the global icehouse conditions at these times (Ahlborn and Stemmerik 2015; Smyrak-Sikora *et al.* 2019, 2021). A more detailed description of TSE 2 is available in Supplementary material 1.

TSE 3: upper Moscovian–Lower Permian upper Gipsdalen Group. The upper Pennsylvanian and Lower Permian successions represent a distinctive element in the evolution of the SCTSE with the development of an extensive and long-lived carbonate platform, reflecting a combination of regional subsidence, waning extensional tectonics and eustatic sea level (Stemmerik and Worsley 2005).

Strata included in the Moscovian–lower Sakmarian part of the Gipsdalen Group are assigned to the Wordiekammen Formation, which formed a shallow-marine carbonate platform across the SCTSE. Condensed and amalgamated shallow-marine facies successions dominate across the underlying structural highs such as the well-studied eastern Nordfjorden High (Fig. 6). Thicker, non-amalgamated successions dominate in areas overlying the previous rift-basin centre (Ahlborn and Stemmerik 2015; Sorento *et al.* 2020). Deposition at this time was also strongly influenced by frequent, high-amplitude glacio-eustatically driven relative sea-level fluctuations governed by waxing and waning of ice sheets in the southern hemisphere. A more detailed description of TSE 3 is available in Supplementary material 2.

TSE 4: upper Lower–Upper Permian Tempelfjorden Group. Deposits of the Gipshuken Formation reflect a transition from gypsum deposition in a shallow extensive salina system to deeper, cooler-water carbonate shelf deposition (Sorento *et al.* 2020). The structural control becomes evident in the Artinskian by the uplift of prominent highs such as Nordfjorden High and the Sørkapp–Hornsund High (Hellem 1980; Knag 1980; Matysik *et al.* 2017). The basal Vøringen Member forms a distinctive brachiopod packstone-dominated transgressive sheet-like unit (e.g. Uchman *et al.* 2016). Thickness and facies variations of the Tempelfjorden Group are linked to the Late Permian rift event along the western Barents shelf margin. On the SCTSE, an extensive, cool-water carbonate platform succession developed, assigned to the Tempelfjorden Group (Fig. 4). Spiculites and shale dominates the deeper part of the basin, whereas cool-water carbonates and glauconitic sandstones of shallow-marine (i.e. inner-shelf) origin occur along the basin margins and in the proximity to structural highs (e.g. Blomeier *et al.* 2011, 2013; Bond *et al.* 2017; Uchman *et al.* 2016). Sandstone wedges in the southern part of Spitsbergen are banked onto the Sørkapp–Hornsund High (Knag 1980) and are consistent with an active synrift basin fill. Regional subsidence in combination with a eustatic sea-level rise resulted in deepening of the SCTSE. In addition, continued northward continental drift promoted climatic cooling in concert with globally high-silica production in the oceans. A more detailed description of TSE4 is available in Supplementary material 2.

TSE 5: Triassic–Middle Jurassic Sassendalen and Kapp Toscana groups. The base of the Mesozoic in a shale interval near the base of the Sassendalen Group (Zuchuat *et al.* 2020) marks a regional shift from carbonate and silica/spiculite deposition to siliciclastic deposition across the SCTSE. The Early–Middle Triassic Vardebukta, Tvillingodden and Bravaisberget formations that crop out in western Spitsbergen include coarser-grained, shallow-marine and deltaic wedges that built into the basin from the west (Fig. 4) (Mørk *et al.* 1982; Czarniecka *et al.* 2020). These deposits transition eastwards into offshore mudstones of the Lower Triassic Vikinghøgda Formation and the overlying Botneheia Formation (Fig. 4) (Mørk *et al.* 1999; Vigran *et al.* 2014; Wesenlund *et al.* 2022).

During deposition of the Kapp Toscana Group, the sediment supplied to the SCTSE was mainly sourced from the ESE, recording the distal part of a northwestward-prograding deltaic clinoform system approaching from the Uralian mountains and the northeastern part of the Baltic Shield (Riis *et al.* 2008; Smelror *et al.* 2009; Glørstad-Clark *et al.* 2011; Høy and Lundschien 2011; Klausen *et al.* 2014, 2017, 2019; Gilmullina *et al.* 2021). The northward progradation of this system was initiated during the latest Permian along the Fennoscandian coastline but did not reach the SCTSE before the Ladinian

(Riis *et al.* 2008; Lundschien *et al.* 2014; Lord *et al.* 2017). Local highs throughout the eastern part of the SCTSE existed with the Induan part of the succession missing in many places (Mørk *et al.* 1999; Vigran *et al.* 2014; Lord *et al.* 2017). The prodeltaic part of this delta system is represented by the Tschermakfjellet Formation (Ladinian–early Carnian), whereas the overlying De Geerdalen Formation (Carnian–early Norian) represents distal delta front to delta/coastal deposits (Fig. 4) (Klausen and Mørk 2014; Lord *et al.* 2014, 2017; Rød *et al.* 2014; Anell *et al.* 2020). Growth faults and delta collapse are recorded on the west coast of Edgøya (Edwards 1976; Smyrak-Sikora *et al.* 2020). Facies become generally more sandstone rich and increasingly more proximal in the eastern part of the SCTSE (e.g. Hopen, Edgeøya, Wilhelmøya and Barentsøya) than in Spitsbergen (Mørk *et al.* 1982; Lord *et al.* 2017). In the upper part of the formation in Spitsbergen and on Wilhelmøya, the Isfjorden Member consists of heterolithic, intercalated beds of shale, siltstone and sandstone. Red beds with immature to decimetre-thick mature calcrete soil profiles (i.e. hard pans) interbedded with 1–2 m-thick mouth-bar and meandering channel deposits are present, as are calcareous and non-calcareous soil profiles giving the unit a distinctive red and green coloration (Lord *et al.* 2022). These facies indicate that the Isfjorden Member represents a delta-top environment. These more condensed successions and prevalent localized subaerial exposure surfaces at the top of the De Geerdalen Formation are consistent with a proposed reduction in subsidence at the transition to the Norian and Early Jurassic (cf. Ryseth 2014). On Hopen to the SE in the SCTSE, the Hopen Member represents a shallow-marine interval that can be traced east of Svalbard (Lundschien *et al.* 2014). This is likely to indicate early onset of basin sag and the development of a seaway in this area prior to the Norian flooding at the base of the Wilhelmøya Subgroup. It is presently unclear whether the Hopen and Isfjorden members are time-equivalent units as extensive erosion at the base of the Wilhelmøya Subgroup has recently been reported and the unit may simply be absent on Spitsbergen (Hounslow *et al.* 2022; Klausen *et al.* 2022).

The basal boundary of the lower Norian–lower Bathonian Wilhelmøya Subgroup represents a regional unconformity surface overlain by the conglomeratic Slottet Bed that was deposited during a pan-Arctic Norian flooding event (cf. Embry 1997). In the SCTSE, the basal boundary of the Wilhelmøya Subgroup also marks a change from immature sandstones to more quartz-rich sandstones (Mørk 2013; Lord *et al.* 2019), possibly recording a regional change in the provenance area and the reworking of older sedimentary rocks in concert with a change from semi-arid to more humid climatic conditions.

The Wilhelmøya Subgroup is subdivided into three formations, where the lower mudstone-dominated Flatsalen Formation represents widespread prograding offshore to delta-front deposits. A major subaerial sequence boundary occurs near the base of the Rhaetian, informally referred to as 'the Rhaetian unconformity' (cf. Embry 2009; Lord *et al.* 2019). While the Rhaetian–Pliensbachian paralic Svenskøya Formation comprises an almost 200 m-thick succession in Kong Karls Land, it forms a 5–20 m-thick condensed, shallow-marine succession with numerous hiatuses in central and western Spitsbergen (Olaussen *et al.* 2018; Rismyhr *et al.* 2018). Similar thickness trends and hiatuses occur in the SWBS (e.g. Müller *et al.* 2019). It has been suggested that both trends are linked to the tectonism of the Novaya Zemlya Orogen (Klausen *et al.* 2022). By the Toarcian, the variations in thickness were mostly levelled out throughout the archipelago. The upper part of the Wilhelmøya Subgroup is represented by the widespread Toarcian–Bathonian Kongsøya Formation. This formation is highly condensed and dominated by shoreface deposits, commonly separated by offshore sandstones and shales. The uppermost unit of the Kongsøya Formation is the Bathonian Brentskardhaugen Bed (Fig. 4). It represents a regional transgression and is composed of a polymictic phosphatic conglomerate containing reworked Toarcian–?Bajocian fossils (Bäckström and Nagy 1985; Rismyhr *et al.* 2018). A more detailed description of TSE 5 is available in Supplementary material 3.

TSE 6: Middle Jurassic–Lower Cretaceous Adventdalen Group. The group records other dramatic switches in palaeodrainage and source area related to uplift in the west and NW of Svalbard, and later volcanic activity in the north and to the east.

Organic-rich shales in the Agardhfjellet Formation (Fig. 4) were deposited on a shallow shelf under variable oxic, dysoxic and anoxic seafloor conditions (Nagy *et al.* 2009). Distal delta-front or lower-shoreface deposits occur within the otherwise shale-dominated unit in western Spitsbergen, recording the initial arrival of sediments sourced from terranes NW and west of Spitsbergen (Dypvik and Zakharov 2012; Koevoets *et al.* 2018). The Slottsmøya Member, the uppermost member of the Agardhfjellet Formation, has recently emerged as one of the world's richest sources of Jurassic ichthyosaur and plesiosaur fossils (Delsett *et al.* 2016).

The overlying upper Ryazanian/Valanginian–lower Barremian Rurikfjellet Formation forms a 200–300 m-thick coarsening- and shallowing-upward succession (Grundvåg *et al.* 2019; Jelby *et al.* 2020; Śliwińska *et al.* 2020). A basal, condensed glauconitic clay unit – the Myklegardfjellet Bed – formed during maximum flooding of the shelf (Dypvik *et al.* 1992) and represents the onshore equivalent of similar-aged, condensed carbonates of the Klippfisk Formation offshore, whose base is defined by the Base Cretaceous Unconformity (Smelror *et al.* 1998). The lower part of the Rurikfjellet Formation is shale dominated and represents deposition on an open-marine shelf (Grundvåg *et al.* 2017, 2019). Thick successions of gravity-flow deposits occur locally in the NW (Grundvåg *et al.* 2019). The upper part of the formation consists of shallow-marine to deltaic sandstones forming two separate wedges: central and southern Spitsbergen, respectively (Dypvik *et al.* 1991; Grundvåg and Olaussen 2017; Grundvåg *et al.* 2019; Jelby *et al.* 2020).

The overlying up to 120 m-thick fluvio-deltaic succession is assigned to the Barremian–lower Aptian Helvetiafjellet Formation (Fig. 4) (Midtkandal and Nystuen 2009; Grundvåg *et al.* 2017, 2019). The lower part consists of a regionally extensive, cross-bedded sandstone sheet of braided stream affinity (i.e. the Festningen Member), which locally fills incised valleys. The Helvetiafjellet Formation exhibits a transgressive trend, with fluvial deposits in the lower part being overlain by coastal/delta-plain barrier and wave-dominated delta-front sandstones (Nemec *et al.* 1988; Grundvåg *et al.* 2019). The main source area for this fluvio-deltaic system was the exhumed terranes north and west of the SCTSE with depocentres on the shelf further to the south and SE (Gjelberg and Steel 1995; Midtkandal and Nystuen 2009; Grundvåg and Olaussen 2017). A regional provenance switch, however, is documented in the middle part of the formation attributed to the emerging volcanic terrains of the HALIP to the east (Edwards 1979; Maher 2001; Maher *et al.* 2004).

The conformably overlying Carolinefjellet Formation of early Aptian–late middle Albian age is up to 1200 m thick and represents the youngest preserved Mesozoic strata in Svalbard (Fig. 4) (Maher *et al.* 2004; Grundvåg *et al.* 2019, 2020). The base of the formation is defined by a regionally extensive lower Aptian organic-rich shale unit deposited during the final drowning of the retreating Helvetiafjellet Formation delta (Midtkandal *et al.* 2016; Grundvåg *et al.* 2019). The remaining part of the Carolinefjellet Formation was generally deposited

in an open-marine, storm-dominated shelf setting, and consists of alternating inner-shelf sandstone sheets and offshore mudstone units (Grundvåg *et al.* 2020). A more detailed description of TSE 6 is available in Supplementary material 4.

TSE 7: Paleocene–Eocene Van Mijenfjorden Group. The up to 1.9 km-thick Paleogene Van Mijenfjorden Group in the CTB consists of a Paleocene and an Eocene to possibly Early Oligocene succession.

Bentonite (tephra) layers sampled from the Firkanten, Frysjaodden and Basilika formations in the CTB yield U–Pb ages of 61.6, 59.3 and 55.8 Ma, respectively (Charles *et al.* 2011; Jones *et al.* 2017; Jochmann *et al.* 2020). The oldest bentonite bed, at the base of the Firkanten Formation, can be traced laterally for almost 100 km from north to south within the basin (Jochmann *et al.* 2020). Geochemical fingerprinting suggests the Kapp Washington volcanic rocks in North Greenland as the source for the oldest bentonite bed, while the younger beds are likely to represent volcanism in the Nares Strait, Arctic Canada (Jones *et al.* 2016, 2017). The youngest dated bentonite in the CTB has been used to refine the absolute age of the Paleocene–Eocene Thermal Maximum (PETM: Charles *et al.* 2011).

The Paleocene succession accumulated in a fault-bounded basin, and consists of offshore shale (the Basilika Formation) and intercalated sandstone wedges of shallow-marine to paralic origin (i.e. the Firkanten, Grumantbyen and Hollendardalen formations). The paralic lower part of the Firkanten Formation represents the most important coal-bearing unit in Svalbard (Nøttvedt 1985; Lüthje *et al.* 2020).

The Eocene basin fill accumulated in a foreland basin that formed in response to the development of the WSFTB. It represents an overall regressive megasequence comprising several hundred metres of thick basin-floor shale of the Frysjaodden Formation at the base, gradually passing upwards into shallow-marine to deltaic sandstones of the Battfjellet Formation, and eventually alluvial deposits of the Aspelintoppen Formation (Helland-Hansen 2010; Grundvåg *et al.* 2014*a*; Helland-Hansen and Grundvåg 2020). The Paleocene succession was largely sourced from the east, whereas the overlying Eocene to possible early Oligocene succession saw a major change to westerly derived sediments in response to the growing WSFTB (Steel *et al.* 1985; Helland-Hansen 1990; Bruhn and Steel 2003; Petersen *et al.* 2016).

Paleogene outliers also occur in several smaller structurally confined basins within the WSFTB (e.g. Blinova *et al.* 2013; Smelror and Larssen 2016; Jochmann *et al.* 2020; Schaaf *et al.* 2021). A more detailed description of TSE 7 is available in Supplementary material 5.

Magmatism

Carboniferous

A vertical NE–SE-striking monchiquite (lamprophyre) dyke occurs at Krosspynten in Wijdefjorden, Spitsbergen (Gayer *et al.* 1966). It is approximately 0.9 m wide, and clearly cross-cuts folded Devonian sandstones and shales. It has a vertically zoned appearance with alternating fine- and coarse-grained crystals, and exhibits vertical and horizontal fractures. Krasil'shchikov (1964) obtained a K–Ar age of 309 ± 5 Ma for the dyke, suggesting a Late Carboniferous basic magmatism (Gayer *et al.* 1966). However, an ongoing study, applying the $^{40}Ar/^{39}Ar$ step heating method, indicates an older, possible late Mississippian age for the intrusion (Morgan Ganerød pers. comm. 2019).

Early Cretaceous

In Svalbard, Early Cretaceous mafic rocks related to the HALIP are assigned to the Diabasodden Suite (Dallmann *et al.* 1999; Senger *et al.* 2014*a*, *b*), which comprises both doleritic sills and dykes throughout Svalbard, and basaltic lava flows on Kong Karls Land (Smith *et al.* 1976; Bailey and Rasmussen 1997; Olaussen *et al.* 2018). The intrusions are emplaced in a wide range of lithologies and stratigraphic intervals. In Spitsbergen, Edgeøya and Barentsøya, they are preferentially located in Triassic shales (early phase of TSE 4), whereas further east (i.e. at Kong Karls Land) they appear in Upper Jurassic shales and Lower Cretaceous sandstones (late phase of TSE 4). U–Pb dating of several sills suggests a short-lived magma emplacement pulse at *c.* 124.5 Ma (Corfu *et al.* 2013). On Kong Karls Land, tholeiitic plateau flood basalts are resting on, or interfingering with, the fluvio-deltaic Helvetiafjellet Formation (which at this location is suggested to be of an Aptian age: Smelror *et al.* 2018), and volcanoclastic material locally occurs in fluvial-channel deposits within the unit (Olaussen *et al.* 2018). Ongoing studies using the $^{40}Ar/^{39}Ar$ step heating method gave a maximum age for lava flows of 126.1 ± 1.7 Ma (Morgan Ganerød pers. comm. 2020).

Heat flow

The current geothermal gradient and heat flow vary from 25 to 55°C km^{-1} and from 65 to 70 W m^{-2}, respectively (Fig. 7) (Betlem *et al.* 2018). The base of the Paleocene Firkanten Formation in the central parts of the CTB were subjected to temperatures of 120°C, reflecting a geothermal gradient of approximately 50°C km^{-1} in the Eocene–Oligocene. The local variations in geothermal conditions across the archipelago, at least partially, may be explained by the present out-of-equilibrium conditions due to Neogene pre-glacial and glacial loading, unloading, and erosion rates (Lucazeau 2019).

Localized Neogene–Quaternary volcanism reported in northwestern Spitsbergen (Dallmann 2015), fluid migration along pre-existing fault zones and effects from the asthenosphere (e.g. Minakov 2018) may all have contributed to the documented thermal heterogeneity.

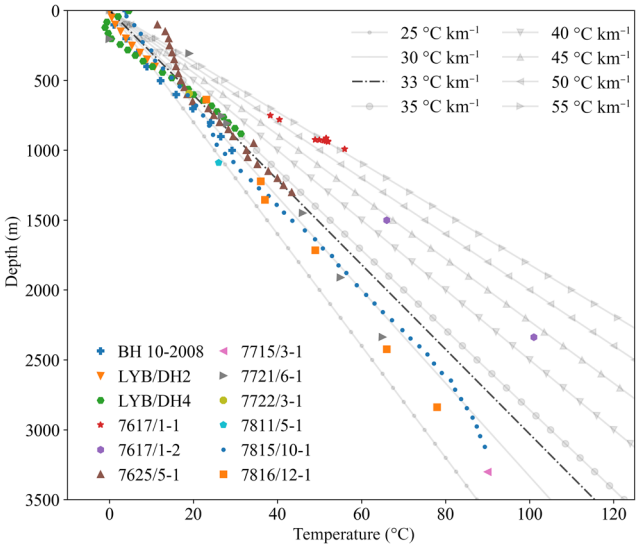

Fig. 7. Temperature gradients from exploration and research wells.

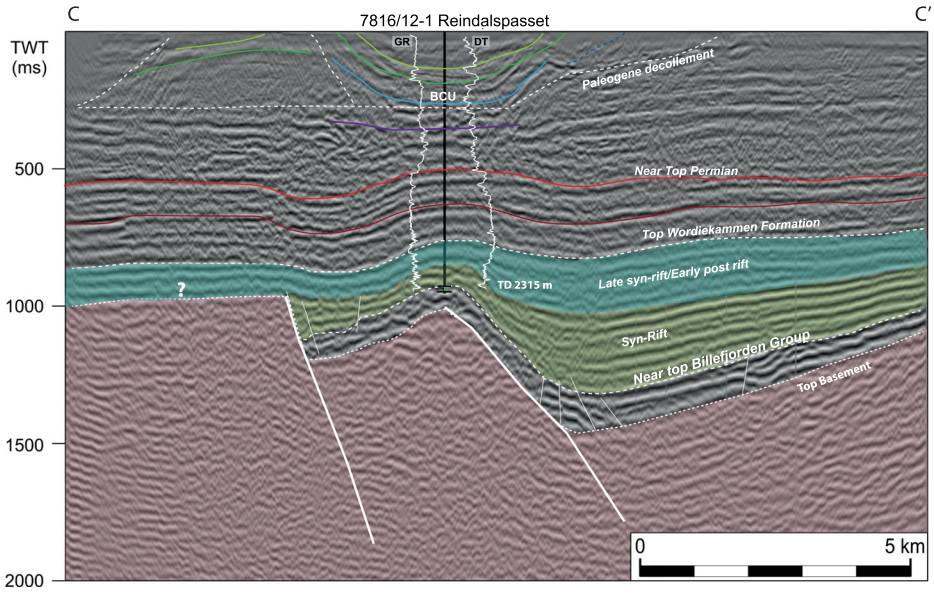

Fig. 8. The only example of a drilled prospect based on subsurface mapping in Svalbard, Reindalspasset, well 7816/12-1. The target was a play with a Pennsylvanian rotated fault block as the trap, and sandstone and carbonates as the reservoir, which were sourced from Mississippian coal and shales. BCU, Base Cretaceous Unconformity (i.e. Base Rurikfjellet Formation); TD, terminal depth; TWT, two-way travel time. Colour legend for the seismic reflectors: brown, intra-Permian reflector; red, near top Permian (i.e. top Kapp Starostin Formation); violet blue, BCU; dark green, Base Helvetiafjellet Formation; light green, base Carolinefjellet Formation. See Figure 4 for the stratigraphy.

Petroleum geology

Discovered and potential petroleum resources

No economic discoveries have been made onshore Svalbard, although small technical discoveries are reported from oil and gas exploration, coal exploration, and scientific drilling (Senger *et al.* 2019). Most drilled prospects in Svalbard were de-risked based on the surface geology, mapping and stratigraphy. The exception to this is the 7816/12-1 Reindalspasset well, which drilled a prospect defined on 2D seismic data (Fig. 8).

Current exploration status

There has been no hydrocarbon exploration in the Svalbard archipelago or the surrounding territorial waters (12 nm from the coastline) since 1995. The very high technical risk of making economic discoveries is combined with several logistical challenges: the remoteness of the high Arctic, strict environmental regulations and numerous protected areas throughout the archipelago. Because of this, any future exploration in the archipelago is inconceivable.

Hydrocarbon systems and plays

Although there are no indications of economically valuable oil or gas accumulations in the SCTSE, unconventional hydrocarbons in the form of shale gas have been proven in the Agardhfjellet Formation in Adventdalen in the vicinity of Longyearbyen, possibly representing a local energy source for the future (Ohm *et al.* 2019). Bituminous-stained sandstones and carbonates occurring in several stratigraphic levels of the SCTSE indicate the presence of multiple source rocks and migration phases that record secondary oil migration and dismigration into previously efficient traps (Fig. 4). Palaeohydrocarbon accumulations sourced from Carboniferous and Lower Permian lacustrine mudstones, coals and carbonates (TSE 1 and TSE 2) have probably been efficiently sealed by mudstones or evaporites in central parts of the archipelago (Nicolaisen *et al.* 2019). Furthermore, recent studies of bitumen-stained Mesozoic sandstones (Abay *et al.* 2017) suggest that oil has migrated from the organic-rich mudstones of the Middle Triassic Botneheia Formation (TSE 5) and the Middle Jurassic–Lower Cretaceous Agardhfjellet Formation (TSE 6). The first phase of migration from these Mesozoic source rocks and the succeeding accumulation in porous sandstones probably occurred prior to the regional Neogene uplift. This palaeohydrocarbon system is analogous to age-equivalent, prolific plays in the SWBS, where the Steinkobbe and Hekkingen formations act as source rocks. Discovery of non-biodegraded bituminous sandstones in the Lower Jurassic Svenskøya Formation (lower part of TSE 4) on the east coast of Spitsbergen also points to a second, and more recent, migration phase, probably related to late Neogene uplift and erosion (Abay *et al.* 2017). Roy *et al.* (2019) documented ongoing near-shore gas seepage in northern Isfjorden, while Hodson *et al.* (2020) illustrated methane seepage through pingos onshore Nordenskiöld Land. In many places throughout Svalbard, gas accumulations have been trapped at the base of permafrost. At Kapp Amsterdam near Svea, a significant shallow gas accumulation at the base of permafrost was encountered in a terminal moraine that is only 600 years old – also evidence of ongoing hydrocarbon migration at present. The out-of-equilibrium system may also result in hard-to-predict hydrodynamically trapped hydrocarbon accumulations.

A major factor of the hydrocarbon system in the SCTSE is the pore pressure. Due to the out-of-equilibrium conditions, the pore-pressure regimes are diverse throughout Svalbard, ranging from severe underpressure to mild overpressure. While the overpressure can be explained by topography-driven flow or gas buoyancy, the more severe cases of underpressure cannot. The most reliable quantitative pressure data are derived from the Longyearbyen CO_2 Lab boreholes in Adventdalen (Braathen *et al.* 2012; Olaussen *et al.* 2019), where long-term pressures were recorded (Birchall *et al.* 2020). Parts of the Mesozoic succession are severely underpressured, with pressures up to 60 bar below hydrostatic recorded in the Wilhemøya Subgroup and in the lower parts of the regional cap-rock unit, the Agardhfjellet Formation (Fig. 4) (Birchall *et al.* 2020). Studies show that this condition formed recently and is in a state of disequilibrium (Wangen *et al.* 2016; Birchall *et al.* 2020). These geologically recent changes in pressure–volume–temperature (PVT) conditions almost certainly promote active ongoing migration (Birchall *et al.* 2020), which is also supported by numerous seeps, flares and shows throughout the archipelago (Senger *et al.* 2019 and references therein).

Source rocks. Source-rock units occur at multiple stratigraphic levels within the SCTSE (Fig. 4). Below follows an

overview of the most important and relevant source-rock units, particularly those relevant for exploration in the SWBS.

Carboniferous and Permian (TSE 1–TSE 4). Organic-rich mudstones and coals in the Billefjorden (TSE 1) and Gipsdalen (TSE 2 and TSE 3) groups are proven potential source rock units in central Spitsbergen (van Koeverden *et al.* 2011; Nicolaisen *et al.* 2019). A normal distribution of T_{max} of 440°C suggests maturation in the late oil window (Nicolaisen *et al.* 2019). Coaly mudstones and organic-rich floodplain deposits to lacustrine mudstone in the Mississippian Billefjorden Group in central Spitsbergen have reported total organic carbon (TOC) values of 11–28 wt%, and a hydrogen index (HI) of *c.* 160–350 mgHC g^{-1} TOC, and a mixture of Type II and III kerogen. These fine-grained organic-rich units might add up to *c.* 100 m in cumulative thickness. The interbedded coal seams yield both gas and oil (Abdullah *et al.* 1988; van Koeverden and Karlsen 2011).

Organic-rich marine calcareous mudstones in the Gipsdalen Group occur as either thin beds intersecting carbonates or evaporites, or as a thicker (up to 10 m) unit of fusulinid-rich shaly limestone: the Lower Permian Brucebyen Bed (Nicolaisen *et al.* 2019). The thin interbeds have an average TOC of 1–10 wt% and HI values of 200–400 mgHC g^{-1} TOC. The beds seldom reach a thickness above 30–40 cm but might add up to *c.* 10 m in the Minkinfjellet and Gipshuken formations. In comparison, the Brucebyen Bed reach an average TOC of 2.4 wt% and a HI index ranging from 100 to 350 mgHC g^{-1} TOC (Nicolaisen *et al.* 2019), thus forming the most significant source rock in the Gipsdalen Group.

Mesozoic (TSE 5 and TSE 6). The two most important regional source rocks in the SCTSE are the organic-rich marine mudstone (OMM) from the Middle Triassic Botneheia Formation (TSE 5) and the Middle Jurassic–Lower Cretaceous Agardhfjellet Formation (TSE 6). Their offshore near time-equivalent counterparts, the Steinkobbe and Hekkingen formations, respectively, are both known to charge numerous fields in the Norwegian Barents Sea (Leith *et al.* 1993; Ohm *et al.* 2008; Henriksen *et al.* 2011*b*; Abay *et al.* 2018). Both the Botneheia and Agardhfjellet formations were deposited in relatively shallow shelf waters, periodically under anoxic seafloor conditions, in distal prodeltaic settings in front of large, prograding delta systems (Glørstad-Clark *et al.* 2011; Anell *et al.* 2014*a*, *c*, 2016; Koevoets *et al.* 2018; Wesenlund *et al.* 2022). Bitumen in Mesozoic sandstones from outcrops and cored boreholes indicate that both OMM units were once active source rocks (Abay *et al.* 2017). The maturation of the Mesozoic OMM within the SCTSE records a west–east trend from burned out/overmature in the SW to late oil window in the west via peak oil window in central parts to immature in the east. The same trend is seen in the sandstone diagenesis from tight in the west and south to unconsolidated Mesozoic sand on Kong Karls Land to the east. These trends are shown in Figure 9. Local intrusive Cretaceous volcanic rocks may influence this trend (Senger *et al.* 2013; Brekke *et al.* 2014; Olaussen *et al.* 2018).

The Botneheia Formation ranges from 80 to 160 m in thickness, and contains dominantly kerogen type II in its upper part and type III in its lower part, with TOC values ranging from *c.* 1 to 11 wt%, with the Blanknuten Member in the upper part of the formation exhibiting the highest organic content (Mørk and Bjorøy 1984; Krajewski 2013; Wesenlund *et al.* 2021, 2022). On NW Edgeøya and south Barentsøya, this part of the formation is in the oil window (Fig. 9) and is an excellent potential oil-prone source rock with q median TOC value of 8.10 ± 1.06 wt% and a HI value of 538 ± 42 mgHC g^{-1} TOC (Wesenlund *et al.* 2021). This upper member is also typically rich in phosphate, suggesting an influence from upwelling and subsequent high rates of primary production, which eventually promoted oxygen deficiency in the water column (Krajewski 2013; Wesenlund *et al.* 2021). Integrated geochemical studies by Wesenlund *et al.* (2021, 2022) suggest that the lower part of the Botneheia Formation is expected to generate mixed oil and gas (during conditions equivalent to peak oil generation) with relatively greater amounts of saturated v. aromatic hydrocarbons compared to the oil-prone, phosphate-bearing upper part of the unit.

In western Spitsbergen, 20–30 m-thick OMM in the lower part of the Bravaisberget Formation (Fig. 4) is correlative with the Botneheia Formation and may locally hold some source potential (Mørk *et al.* 1999).

The Agardhfjellet Formation is an up to 240 m-thick Bathonian–Ryazanian organic-rich mudstone-dominated formation containing >100 m-thick OMM (accumulative) with a TOC that ranges from 2 to 15% (Hvoslef *et al.* 1986; Leith *et al.* 1993; Koevoets *et al.* 2018; Ohm *et al.* 2019).

Core data from Adventdalen, central Spitsbergen, show that the formation contains a mixture of type II and type III kerogen, a TOC of 6–10% and a HI of 50–200 mgHC g^{-1} TOC. T_{max} varies from 275 to 455°C in the black paper shale in the lower part of the Agardhfjellet Formation (Koevoets *et al.* 2016). In the east, the formation is largely missing due to erosion related to Late Jurassic and Early Cretaceous inversion (Grogan *et al.* 1999). However, the lowermost part is immature, with vitrinite reflectance values (VR) of 0.38 to 0.42%, a T_{max} of 410°C and TOC values of up to 40% (Olaussen *et al.* 2018).

Another regionally extensive organic-rich mudstone unit with some source potential occurs in the basal part of the lower Aptian–middle Albian Carolinefjellet Formation (uppermost TSE 4: Fig. 4) on Spitsbergen (Midtkandal *et al.* 2016; Grundvåg *et al.* 2019). This 5–30 m-thick potential source-rock unit accumulated during a regional transgression of the underlying delta plain of the Helvetiafjellet Formation in the early Aptian and was evidently influenced by a global oceanic anoxic event (OAE1a) (Midtkandal *et al.* 2016; Zhang *et al.* 2021). Analyses of core material from central Spitsbergen indicate that this unit is dominated by kerogen type III with TOC values up to 2.1 wt% and a HI of 180 mgHC g^{-1} TOC (Grundvåg *et al.* 2019). An Aptian source-rock unit is proven in the SWBS but here is a potential for oil generation (Hagset *et al.* 2022).

Paleogene (TSE 7). The Paleogene succession in central and western Spitsbergen holds good potential for oil- and gas-prone source rocks, primarily due to the abundance of thick coal seams in the Firkanten Formation (Orheim *et al.* 2007; Marshall *et al.* 2015; Uguna *et al.* 2017). Because of past and ongoing mining, the Paleocene coals have received considerable attention. Maceral analysis of the Firkanten Formation coals document type III kerogen (whereas van Krevelen equivalent diagrams show plots between II and III kerogen) and HI values ranging between 151 and 410 mgHC g^{-1} TOC (Uguna *et al.* 2017). Distillation of coal yields up to 28% crude oil from pure coal (Orvin 1934), whereas recent analysis by hydrous pyrolysis showed a bitumen yield of up to 320 mg g^{-1} TOC (Marshall *et al.* 2015). The bitumen has thus migrated, enriching the upper parts of the investigated coal seams and in part the immediate overlying sandstone (Marshall *et al.* 2015). The coals represent thick accumulations of marine-influenced peat deposits, and have better source-rock potential and oil-generating properties than the closely associated organic-rich floodplain deposits. The coal-bearing strata have locally significant amounts of gas, which were regularly encountered as a hazard during coal

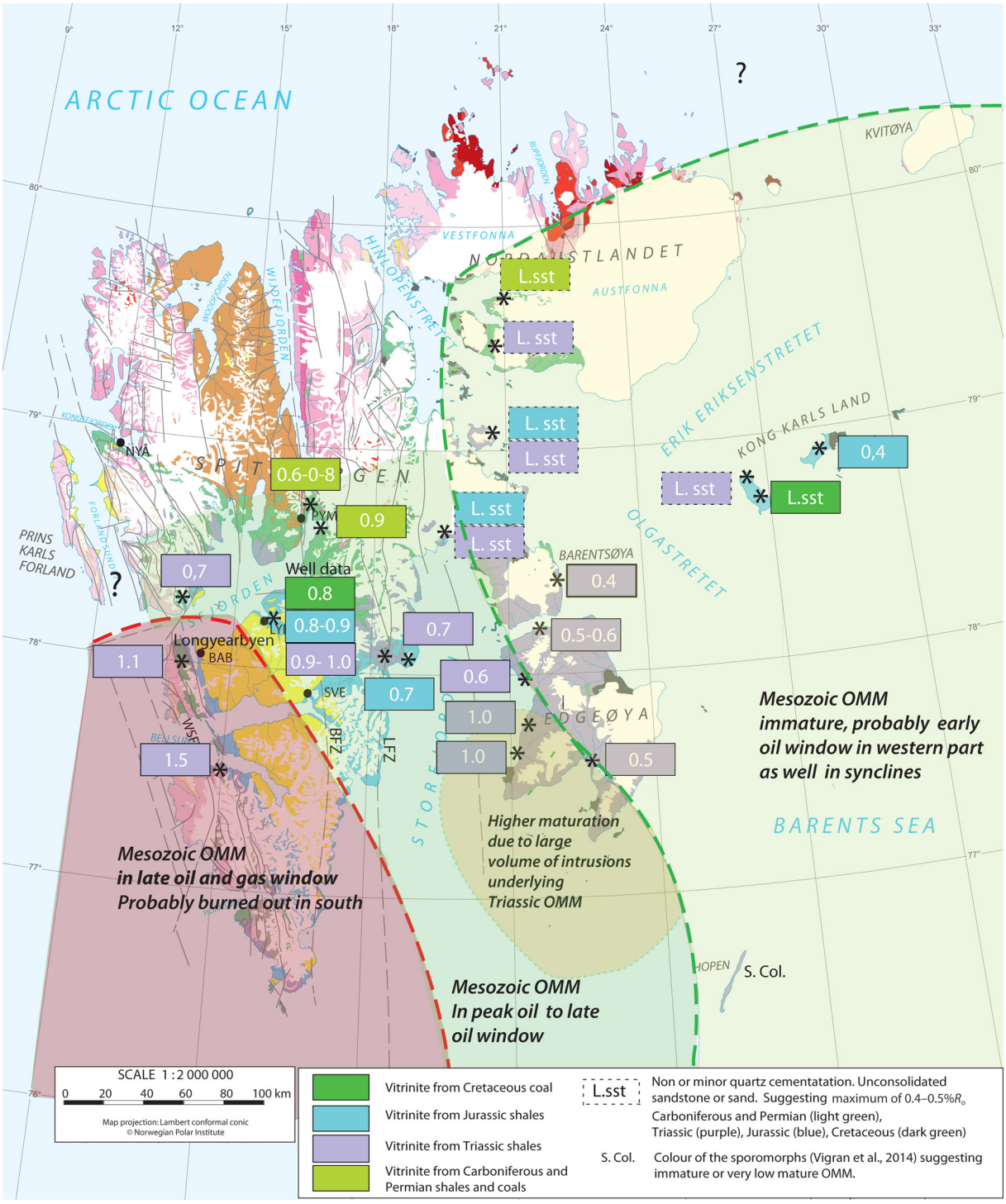

Fig. 9. Maturation trend of Mesozoic organic-rich marine mudstone (OMM) based on the available vitrinite, T_{max}, geochemistry data for bitumen (Mørk and Bjorøy 1984; Abay *et al.* 2017; Ohm *et al.* 2019) and the degree of diagenesis of sandstones (Mørk 2013; Haile *et al.* 2018, 2021), degree of quartz cementation v. maturation (cf., Walderhaug 1996; Bjørlykke and Jahren 2015). Source: geological map from the Norwegian Polar Institute.

exploration drillings in the past, thus representing risk-management challenges to the local mining industry.

Reservoirs. Potential reservoir rocks occur in several of the TSEs described in this study, spanning the Lower Carboniferous (TSE 1) through the Mesozoic (TSE 4) to the Paleogene successions (TSE 5). Based on maturation trends of organic-rich mudstones or coal, the porosity and, in part, the permeability trends of the Upper Paleozoic and Mesozoic sandstones are predictable. The highly diverse reservoirs range from unconventional reservoir units consisting of fractured tight sandstone in the west (e.g. previously deeply buried below the CTB) to poorly unconsolidated sandstone and unconsolidated sand in the easternmost areas (Mørk 2013; Haile *et al.* 2018; Olaussen *et al.* 2018). Upper Carboniferous–Permian carbonate and silica-rich deposits (TSE 3 and TSE 4) are less predictable in an east–west trend, and are largely dependent on the depositional environment, the chemical history of the fluids (related to the burial and uplift history), karstification and dolomitization (Stemmerik and Worsley 1995; Ehrenberg *et al.* 2001; Blomeier *et al.* 2009; Sorento *et al.* 2020). Triassic sandstones (TSE 4) in the east potentially exhibit moderate porosities (12–18%) but low

permeabilities due to poor sorting, immature mineralogy, pore-filling clay minerals and common carbonate cementation.

Carboniferous–Permian (TSE 1–TSE 4). In TSE 1, potential reservoir rocks include various alluvial/fluvial to lacustrine and paralic sandstone units of the Billefjorden Group. The sandstone/shale ratio is highly variable, typically ranging from 0.2 to 0.5. However, higher values are recorded in sandstones up to 100 m thick in the area around the Billefjorden Trough and in the >700 m-thick Orustdalen Formation in west Spitsbergen.

The distribution of reservoir units in TSE 2 is best documented in the Billefjorden Trough. Individual reservoir bodies are typically 10–12 m thick, consisting of fine- to coarse-grained sandstones of paralic origin, and include meandering fluvial-channel fills and braidplain deposits overlain by shoreline and delta-front sandstone units and alluvial fans banked to the master faults (Johannessen and Steel 1992; Braathen *et al.* 2011; Smyrak-Sikora *et al.* 2019).

Potential carbonate reservoir units include >10 m-thick oolitic grainstone units of the Minkinfjellet Formation, which occur along the basin margins and accumulated during the final phase of rifting. Secondary breccias linked to a later event of evaporite dissolution also hold some reservoir potential (Eliassen and Talbot 2005).

The platform carbonates of the Gipsdalen Group have good visible porosity (Ahlborn and Stemmerik 2015). The best porosity, up to 20%, is recorded in carbonate build-ups of localized distribution and considerably less rock volume than in their offshore counterpart in the Ørn Formation in the SWBS (Larssen *et al.* 2002). In the middle part of TSE 3, corresponding to the Gipshuken Formation (Figs 4 & 9), good visible vuggy, mouldic and cavernous porosity is present in the platform carbonates, and dissolution breccias can be traced laterally for several kilometres, in amongst others in the Lomfjorden area. Petrographical analyses have documented both inter- and intra-particle porosities of 15–17% in grainstones and intra-crystalline porosity of 20% in dolomites. The porous platform units are sheet like and persist laterally over several kilometres. The Upper Permian, spiculitic, part of TSE 3 has undergone a complex diagenetic transformation that locally resulted in units with porosities (at best) of up to 12–25% and permeabilities of up to 100 mD (Ehrenberg *et al.* 2001; Matysik *et al.* 2017). Localized Upper Permian glauconitic sandstones occurring along the basin margin may hold some potential, as they are sporadic and seen as partly unconsolidated.

Triassic–Middle Jurassic (TSE 5). The Lower Triassic Vardebukta Formation in the eastern part of the SCTSE features an upwards-coarsening parasequence that terminates in a series of upper-shoreface to fluvial-channel units that may provide good reservoir properties (Mørk *et al.* 1982).

The key Triassic reservoir interval occurs in the De Geerdalen Formation. The sandstone/shale net-to-gross (N/G) of the De Geerdalen Formation (and the age- and facies-equivalent Snadd Formation offshore) increases significantly to the east and SE throughout the SCTSE, reflecting more proximal settings in those directions. Hopen is a key area in highlighting the nature of the Late Triassic reservoir interval throughout the SCTSE and its equivalent units in the Barents Sea (Klausen and Mørk 2014). The well-preserved fluvial-channel-fill sandstone bodies are prominently exposed in the steep cliff sides of the island. Whilst these are relatively isolated in their stratigraphic position and are encased in a highly heterolithic succession, they clearly indicate the presence of relatively good reservoir-quality rocks in the region (Lord *et al.* 2014, 2017).

The Wilhelmøya Subgroup is the onshore analogue to the most prolific hydrocarbon reservoir in the SWBS (i.e. the Realgrunnen Subgroup: Worsley 2008). On Spitsbergen, the Wilhelmøya Subgroup forms a thin Norian–Bathonian condensed paralic sandstone unit, typically <20 m thick, 'tight' sandstone and with numerous hiatuses (Bäckström and Nagy 1985; Rismyhr *et al.* 2018:). This subgroup has been suggested to be a potential CO_2 storage unit, forming an unconventional reservoir that relies on a permeable fracture system (Braathen *et al.* 2012; Ogata *et al.* 2012, 2014; Senger *et al.* 2015; Mulrooney *et al.* 2018; Olaussen *et al.* 2019).

In the eastern SCTSE (i.e. Kong Karls Land), the Wilhelmøya Subgroup thickens to *c.* 200 m. Here, the reservoir sandstones are poorly consolidated, occasionally occurring as loose sand, and appear to be porous and permeable (Olaussen *et al.* 2018). The preserved strata are comparable to the age- and facies-equivalent Realgrunnen Subgroup offshore. The Flatsalen Formation, which is partly analogous to the Fruholmen Formation offshore, has no reservoir potential in Spitsbergen but may hold some potential in eastern Svalbard, with a 0.2–0.3 N/G sandstone/shale ratio. The overlying amalgamated 12–30 m-thick channelized Norian–Rhaetian part of the Sjøgrenfjellet Member of the Svenskøya Formation in Kong Karls Land and Hopen has good reservoir potential with an estimated sandstone/shale ratio of 0.9–1 (Lord *et al.* 2019). The remaining part of the heterolithic deposits of the Hettangian–lower Pliensbachian Sjøgrenfjellet Member shows a variation in the sandstone/shale ratio, ranging from 0.5 to 0.7.

The 20–50 m-thick upper Pliensbachian–upper Toarcian Mohnhøgda Member of the Svenskøya and the upper Toarcian–Aalenian Kongsøya Formation shows a sandstone/shale ratio that ranges from 1 in central Spitsbergen to 0.7–0.8 in the east. On the islands of Kong Karls Land, sandstones of the Kongsøya Formation shale-out towards the east (i.e. from Kongsøya to Svenskøya). This also indicates in a prominent palaeodrainage shift towards a source located more to the east.

Middle Jurassic–Lower Cretaceous (TSE 6). In western Spitsbergen, the Kimmeridgian Oppdalsåta Member of the Agardhfjellet Formation comprises four or five 10–15 m-thick shallowing-upward sequences with a sandstone/shale ratio ranging from 0.3 to 0.5 and visible porosity (Koevoets *et al.* 2018).

In southern Spitsbergen, the Valanginian–Barremian Rurikfjellet Formation may offer some reservoir potential, as its upper part contains a *c.* 150 m-thick succession of stacked coarsening-upward delta-front units. This succession appears to continue southwards into the offshore area of the SCTSE (Grundvåg and Olaussen 2017). We estimate that the sandstone/shale ratio of this succession in the south ranges from *c.* 0.5 in its lower part to 0.8 in its upper part.

One of the most prominent sandstone units in Spitsbergen and Kong Karls Land is the fluvio-deltaic Barremian–Aptian Helvetiafjellet Formation (Fig. 4). The thickness of the unit varies from 45 to >150 m, reflecting deposition within large-scale incised valleys (Gjelberg and Steel 1995; Midtkandal *et al.* 2008; Midtkandal and Nystuen 2009; Olaussen *et al.* 2018; Grundvåg *et al.* 2019), as well as syntectonic movements in the Barremian (Nemec *et al.* 1988; Onderdonk and Midtkandal 2010). The lowermost sandstone unit, the Festningen Member, is a regionally extensive 5–15 m-thick cross-bedded sandstone sheet of braidplain origin. The sandstone/shale ratio is generally high, ranging from 0.6 to 0.9.

Despite low porosities of 6–8% in central Spitsbergen, measured permeabilities are remarkably high (*c.* 80–100 mD) as demonstrated by aquifer flow from this interval during drilling of the Longyearbyen CO2 Lab (Braathen *et al.* 2012) and in

numerous coal exploration boreholes in the Longyearbyen vicinity. The overlying Carolinefjellet Formation contains some sandstone-dominated intervals of mostly shallow-marine origin (Grundvåg *et al.* 2020). However, their reservoir potential is strongly hampered by early diagenetic calcite cementation (Maher *et al.* 2004) and various carbonates precipitated during deeper burial.

Paleogene (TSE 7). In TSE 7, the nearly 2 km-thick Van Mijenfjorden Group in the CTB (Fig. 4) contains several units with reservoir potential, although visible porosity is generally very low.

The lowermost reservoir unit is the 100–170 m-thick Firkanten Formation (Paleocene) that exhibits both shoestring and sheet-like reservoir bodies deposited in a paralic depositional environment. There is an upward increase in the N/G ratio corresponding to a transition from a heterolithic fluvial succession in the lower part to shoreface sandstones with a N/G ratio of 0.9 in the upper part. The Hollendardalen Formation (uppermost Paleocene–lowermost Eocene) forms an up to 150 m-thick, eastward-thinning tidally influenced deltaic wedge confined to the western margin of the CTB. Internally, the wedge is organized into *c.* 10 m-thick coarsening-upward units with a particularly high sandstone/shale ratio in their upper parts.

The Battfjellet Formation and the overlying Aspelintoppen Formation (Eocene to possibly Oligocene?) also hold some reservoir potential. The main reservoir bodies of the Battfjellet Formation comprise a series of shingled, shallow-marine to deltaic units representing a southeastward-prograding shelf-prism clinoform system (Grundvåg *et al.* 2014*a*; Helland-Hansen and Grundvåg 2020). Sandstone-rich turbidite deposits (with high N/G ratios) encased in basin-floor mudstones (i.e. the Frysjaodden Formation) may offer the possibility of stratigraphic traps (Grundvåg *et al.* 2014*b*; Spychala *et al.* 2021). Reservoir units of the Aspelintoppen Formation consist of ribbon-shaped fluvial-channel sandstone bodies and crevasse splay units encased in overbank fines (Grundvåg *et al.* 2014*a*).

Seals. Conventional seals are offered by Paleozoic carbonates and evaporites, thick black shales in the Triassic–Jurassic, and silty shales in the Cretaceous–Paleogene (Fig. 4) (Nøttvedt *et al.* 1993). The sealing capability of potential sealing rocks in the SCTSE is complicated by their laterally heterogenous nature and recent uplift.

The sequence of the Hekkingen and Fuglen formations provides the most important cap rock in the Barents Sea (Ohm *et al.* 2008; Paulsen *et al.* 2022). In Svalbard, the Agardhfjellet Formation forms a time-equivalent cap rock; this is fully cored by four research boreholes of the Longyearbyen CO2 Lab in Adventdalen, and has previously been characterized in terms of sedimentology, mineralogy and geochemistry (Koevoets *et al.* 2016, 2018; Abay *et al.* 2017; Ohm *et al.* 2019).

The rheological impacts of Cenozoic uplift may be profound in cap-rock effectiveness. Previous deep burial has left the potential seals mechanically and chemically overcompacted for their present-day depths. This may enhance some mechanical properties, as is evident from the extremely high leak-off pressures in the Fuglen Formation offshore (Paulsen *et al.* 2022), often more that the lithostatic pressure. Conversely, it may also make the cap rock more prone to brittle failure, with fault zones being a particular risk (Paulsen *et al.* 2022).

Additional possible seals may be offered by faults, igneous intrusions, diagenetic tight sedimentary rocks, evaporites, permafrost and associated gas hydrates (Senger *et al.* 2013; Mulrooney *et al.* 2018; Betlem *et al.* 2019). In particular, permafrost appears to be an efficient shallow seal, as is evident from the thermogenic gas found trapped immediately below the permafrost during several drilling operations in Svalbard.

Migration is obviously ongoing in at least central and eastern parts of Spitsbergen, and is likely elsewhere, as demonstrated by numerous active seeps and flares (Abay *et al.* 2017). The occurrence of a large gas accumulation (and blow-out) below permafrost in moraine sediments that are 600 years old at Kapp Amsterdam also provides evidence of ongoing migration.

Traps. The diverse tectonic history of the SCTSE has resulted in the formation of many potential trapping mechanisms. From extensional faulting in the Paleozoic, producing half-graben or rollover structures, to numerous compression and transpression events, resulting in large gentle anticlines in addition to regional decollement zones (e.g. Nøttvedt *et al.* 1993).

Acknowledgements This review of the Svalbard Composite Tectono-Sedimentary Element is based on many previous works, particularly those led and initiated by the former Harland Group at Cambridge University (UK), and by the research groups at the Norwegian universities in Oslo and Bergen led by David Worsley and Ron Steel, respectively. We thus acknowledge the hard work of previous investigators and are grateful for the framework on which our studies have largely been built. In the 1990s and onwards, research programmes were mostly sponsored by the oil industry, and much of the work presented here would not have been possible without their support. Bjørn Lundschien, Alf Ryseth and Morten Smelror and the editors are gratefully acknowledged for comments that improved the manuscript.

Competing interests The authors declare that they have no known competing financial interests or personal relationships that could have appeared to influence the work reported in this paper.

Author contributions **SO**: supervision (lead), writing – original draft (lead), writing – review & editing (lead); **S-AG**: writing – original draft (equal), writing – review & editing (equal); **KS**: writing – original draft (equal), writing – review & editing (equal); **IA**: writing – original draft (supporting), writing – review & editing (supporting); **PB**: writing – original draft (supporting), writing – review & editing (supporting); **TB**: writing – original draft (supporting), writing – review & editing (supporting); **AB**: writing – original draft (supporting), writing – review & editing (supporting); **WD**: writing – original draft (supporting), writing – review & editing (supporting); **MJ**: writing – original draft (supporting), writing – review & editing (supporting); **EPJ**: writing – original draft (supporting), writing – review & editing (supporting); **GL**: writing – original draft (supporting), writing – review & editing (supporting); **AM**: writing – original draft (supporting), writing – review & editing (supporting); **PTO**: writing – original draft (supporting), writing – review & editing (supporting); **AS-S**: writing – original draft (supporting), writing – review & editing (supporting); **LS**: writing – original draft (supporting), writing – review & editing (supporting).

Funding This work was funded by the Research Council of Norway, which financed the Longyearbyen CO2 Lab, Triassic North (grant no. 234152 awarded to AB), and the ongoing ARCEx (grant no. 228107 to S-AG) and the Suprabasins (grant No. 295208 awarded to AB) projects. Also funded by the industry sponsored Locra/Julocra project awarded to A. Escalona and SO.

Data availability Data sharing is not applicable to this article as no datasets were generated or analysed during the current study.

References

Abay, T.B., Karlsen, D.A., Lerch, B., Olaussen, S., Pedersen, J.H. and Backer-Owe, K. 2017. Migrated petroleum in outcropping Mesozoic sedimentary rocks in Spitsbergen: organic geochemical characterization and implications for regional exploration. *Journalof Petroleum Geology*, **40**, 5–36, https://doi.org/10.1111/jpg.12662

Abay, T.B., Karlsen, D.A., Pedersen, J.H., Olaussen, S. and Backer-Owe, K. 2018. Thermal maturity, hydrocarbon potential and kerogen type of some Triassic to Lower Cretaceous sediments from the southwestern Barents Sea and Svalbard. *Journal of Petroleum Geoscience*, **24**, 349–373, https://doi.org/10.1144/petgeo2017-035

Abdullah, W.H., Murchison, D., Jones, J.M., Telnæs, N. and Gjelberg, J. 1988. Lower Carboniferous coal deposition environments on Svalbard, Svalbard. *Organic Geochemistry*, **13**, 953–964, https://doi.org/10.1016/0146-6380(88)90277-X

Ahlborn, M. and Stemmerik, L. 2015. Depositional evolutionof the Upper Carboniferous–Lower Permian Wordiekammen carbonate platform, Nordfjorden High, central Spitsbergen, Arctic Norway. *Norwegian Journal of Geology*, **95**, 91–126, http://doi.org/10.17850/njg95-1-03

Anell, I., Braathen, A. and Olaussen, S. 2014*a*. The Triassic–Early Jurassic of the northern Barents Shelf: a regional understanding of the Longyearbyen CO_2 reservoir. *Norwegian Journal of Geology*, **94**, 83–98.

Anell, I., Braathen, A. and Olaussen, S. 2014*b*. Regional constraints of the Sørkapp Basin: a Carboniferous relic or a Cretaceous depression. *Marine and Petroleum Geology*, **54**, 123–138, https://doi.org/10.1016/j.marpetgeo.2014.02.023

Anell, I., Midtkandal, I. and Braathen, A. 2014*c*. Trajectory analysis and inferences on geometric relationships of an Early Triassic prograding clinoform succession on the northern Barents Shelf. *Marine and Petroleum Geology*, **54**, 67–179, https://doi.org/10.1016/j.marpetgeo.2014.03.005

Anell, I., Faleide, J.I. and Braathen, A. 2016. Regional tectonosedimentary development of the highs and basins of the northwest Barents Shelf. *Norwegian Journal of Geology*, **96**, 27–41, http://doi.org/10.17850/njg96-1-04

Anell, I., Zuchuat, V. *et al*. 2020. Tidal amplification and along-strike process variability in a mixed-energy paralic system prograding onto a low accommodation shelf, Edgeøya, Svalbard. *Basin Research*, **33**, 478–512, https://doi.org/10.1111/bre.12482

Bäckström, S.A. and Nagy, J. 1985. *Depositional History and Fauna of a Jurassic Phosphorite Conglomerate (the Brentskardhaugen Bed) in Spitsbergen*. Norsk Polarinstitutt Skrifter, **183**.

Bælum, K. and Braathen, A. 2012. Along-strike changes in fault array and rift basin geometry of the Carboniferous Billefjorden Trough, Svalbard, Norway. *Tectonophysics*, **546–547**, 38–55, https://doi.org/10.1016/j.tecto.2012.04.009

Bailey, J.C. and Rasmussen, M.H. 1997. Petrochemistry of Jurassic and Cretaceous tholeiites from Kong Karls Land, Svalbard, and their relation to Mesozoic magmatism in the Arctic. *Polar Research*, **16**, 37–62, https://doi.org/10.3402/polar.v16i1.6624

Beka, T.I., Smirnov, M., Birkelund, Y., Senger, K. and Bergh, S.G. 2016. Analysis and 3D inversion of magnetotelluric crooked profile data from central Svalbard for geothermal application. *Tectonophysics*, **686**, 98–115, https://doi.org/10.1016/j.tecto.2016.07.024

Beka, T.I., Bergh, S.G., Smirnov, M. and Birkelund, Y. 2017*a*. Magnetotelluric signatures of the complex tertiary fold–thrust belt and extensional fault architecture beneath Brøggerhalvøya, Svalbard. *Polar Research*, **36**, 1–14, https://doi.org/10.1080/17518369.2017.1409586

Beka, T.I., Senger, K., Autio, U.A., Smirnov, M. and Birkelund, Y. 2017*b*. Integrated electromagnetic data investigation of a Mesozoic CO_2 storage target reservoir–cap-rock succession, Svalbard. *Journal of Applied Geophysics*, **136**, 417–430, https://doi.org/10.1016/j.jappgeo.2016.11.021

Bergh, S.G., Braathen, A. and Andresen, A. 1997. Interaction of basement-involved and thin-skinned tectonism in the Tertiary fold-and-thrust belt, central Spitsbergen, Svalbard. *AAPG Bulletin*, **81**, 637–661.

Betlem, P., Midttømme, K., Jochmann, M., Senger, K. and Olaussen, S. 2018. Geothermal gradients on Svalbard, Arctic Norway. Abstract presented at the First EAGE/IGA/DGMK Joint Workshop on Deep Geothermal Energy, 8–9 November 2018, Strasbourg, France.

Betlem, P., Senger, K. and Hodson, A. 2019. 3D thermo baric modelling of the gas hydrate stability zone onshore central Spitsbergen, Arctic Norway. *Marine and Petroleum Geology*, **100**, 246–262, https://doi.org/10.1016/j.marpetgeo.2018.10.050

Birchall, T., Senger, K., Harnum, M.T., Olaussen, S. and Braathen, A. 2020. Underpressure in the northern Barents shelf: causes and implications for hydrocarbon exploration. *AAPG Bulletin*, **104**, 2267–2295, https://doi.org/10.1306/02272019146

Bjørlykke, K. and Jahren, J. 2015. Sandstones and sandstone reservoirs. *In*: Bjørlykke, K. (ed.) *Petroleum Geoscience: From Sedimentary Environments to Rock Physics*. Springer, Berlin, 119–149, https://doi.org/10.1007/978-3-642-34132-8_4

Blinova, M., Faleide, J.I., Gabrielsen, R.H. and Mjelde, R. 2013. Analysis of structural trends of sub-sea-floor strata in the Isfjorden area of the West Spitsbergen Fold-and-Thrust Belt based on multichannel seismic data. *Journal of the Geological Society, London*, **170**, 657–668, https://doi.org/10.1144/jgs2012-109

Blomeier, D., Scheibner, C. and Forke, H. 2009. Facies arrangement and cyclostratigraphic architecture of a shallow-marine, warm-water carbonate platform: the Late Carboniferous Ny Friesland Platform in eastern Spitsbergen (Pyefjellet Beds, Wordiekammen Formation, Gipsdalen Group). *Facies*, **55**, 291–324, https://doi.org/10.1007/s10347-008-0163-3

Blomeier, D., Dustria, A., Forke, H. and Scheibner, C. 2011. Environmental change in the Early Permian of NE Svalbard: from a warm-water carbonate platform (Gipshuken Formation) to a temperate, mixed siliciclastic carbonate ramp (Kapp Starostin Formation). *Facies*, **57**, 493–523, https://doi.org/10.1007/s10347-010-0243-z

Blomeier, D., Dustira, A.M., Forke, H. and Scheibner, C. 2013. Facies analysis and depositional environments of a storm-dominated, temperate to cold, mixed siliceous–carbonate ramp: the Permian Kapp Starostin Formation in NE Svalbard. *Norwegian Journal of Geology*, **93**, 75–93.

Bond, D.P., Blomeier, D. *et al*. 2017. Sequence stratigraphy, basin morphology and sea-level history for the Permian Kapp Starostin Formation of Svalbard, Norway. *Geological Magazine*, **155**, 1–17, https://doi.org/10.1017/S0016756816001126

Braathen, A., Bergh, S.G. and Maher, H.D. 1995. Structural outline of a Tertiary Basement-cored uplift/inversion structure in western Spitsbergen, Svalbard: kinematics and controlling factors. *Tectonics*, **14**, 95–119, https://doi.org/10.1029/94TC01677

Braathen, A., Bergh, S.G. and Maher, H.D. 1999. Application of a critical wedge taper model to the Tertiary transpressional fold-thrust belt on Spitsbergen, Svalbard. *GSA Bulletin*, **111**, 1468–1485, https://doi.org/10.1130/0016-7606(1999)111<1468:AOACWT>2.3.CO;2

Braathen, A., Bælum, K., Maher, H. and Buckley, S.J. 2011. Growth of extensional faults and folds during deposition of an evaporite-dominated half-graben basin; the Carboniferous Billefjorden Trough, Svalbard. *Norwegian Journal of Geology*, **91**, 137–161.

Braathen, A., Bælum, K. *et al*. 2012. Longyearbyen CO_2 lab of Svalbard, Norway – first assessment of the sedimentary succession for CO2 storage. *Norwegian Journal of Geology*, **92**, 353–376.

Brekke, T., Krajewski, K.P. and Hubred, J.H. 2014. Organic geochemistry and petrography of thermally altered sections of the Middle Triassic Botneheia Formation on south-western Edgeøya, Svalbard. *Norwegian Petroleum Directorate Bulletin*, **11**, 111–128.

Bruhn, R. and Steel, R. 2003. High-resolution sequence stratigraphy of a clastic foredeep succession (Paleocene, Spitsbergen): An example of peripheralbulge-controlled depositional architecture. *Journal of Sedimentary Research*, **73**, 745–755, https://doi.org/10.1306/012303730745

Charles, A.J., Condon, D.J. *et al*. 2011. Constraints on the numerical age of the Paleocene–Eocene boundary. *Geochemistry, Geophysics, Geosystems*, **12**, Q0AA17, https://doi.org/10.1029/2010GC003426

Clark, S., Glorstad-Clark, E., Faleide, J., Schmid, D., Hartz, E. and Fjeldskaar, W. 2014. Southwest Barents Sea rift basin evolution: comparing results from backstrippingand time-forward modelling. *Basin Research*, **26**, 550–566, https://doi.org/10.1111/bre.12039

Corfu, F., Polteau, S., Planke, S., Faleide, J.I., Svensen, H., Zayoncheck, A. and Stolbov, N. 2013. U–Pb geochronology of Cretaceous magmatism on Svalbard and Franz Josef Land, Barents Sea Large Igneous Province. *Geological Magazine*, **150**, 1127–1135, https://doi.org/10.1017/S0016756813000162

Cutbill, J. and Challinor, A. 1965. Revision of the stratigraphical scheme for the Carboniferous and Permian rocks of Spitsbergen and Bjørnøya. *Geological Magazine*, **102**, 418–439, https://doi.org/10.1017/S0016756800053693

Czarniecka, U., Haile, B.G., Braathen, A., Krajewski, K.P., Kristoffersen, M. and Jokubauskas, P. 2020. Petrography, bulk-rock geochemistry, detrital zircon U–Pb geochronology and Hf isotope analysis for constraining provenance: an example from Middle Triassic deposits (Bravaisberget Formation), Sørkappøya, Svalbard. *Norwegian Journaal of Geology*, **100**, https://doi.org/10.17850/njg100-3-5

Dallmann, W.K. (ed.). 2015. *Geoscience Atlas of Svalbard*. Norsk Polarinstitutt Rapportserie, **148**.

Dallmann, W.K., Birkenmajer, K. *et al*. (eds) 1999. *Lithostratigraphic Lexicon of Svalbard. Review and Recommendations for Nomenclature Use; Upper Palaeozoic to Quaternary Bedrock*. Norsk Polarinstitutt, Tromsø, Norway.

Delsett, L.L., Novis, L.K., Roberts, A.J., Koevoets, M.J., Hammer, Ø, Druckenmiller, P.S. and Hurum, J.H. 2016. The Slottsmøya marine reptile *Lagerstätte*: depositional environments, taphonomy and diagenesis. *Geological Society, London, Special Publications*, **434**, 165–188, https://doi.org/10.1144/SP434.2

Dimakis, P., Braathen, B.I., Faleide, J.I., Elverhøi, A. and Gudlaugsson, S.T. 1998. Cenozoic erosion and the preglacial uplift of the Svalbard–Barents Sea region. *Tectonophysics*, **300**, 311–327, https://doi.org/10.1016/s0040-1951(98)00245-5

Dypvik, H. and Zakharov, V. 2012. Fine-grained epicontinental Arctic sedimentation – mineralogy and geochemistry of shales from the Late Jurassic–Early Cretaceous transition. *Norwegian Journal of Geology*, **92**, 65–87.

Dypvik, H., Nagy, J. *et al*. 1991. The Janusfjellet subgroup (Bathonian to Hauterivian) on central Spitsbergen – a revised lithostratigraphy. *Polar Research*, **9**, 21–43, https://doi.org/10.1111/j.1751-8369.1991.tb00400.x

Dypvik, H., Nagy, J. and Krinsley, D. 1992. Origin of the Myklegardfjellet Bed, a basal Cretaceous marker on Spitsbergen. *Polar Research*, **11**, 21–31, https://doi.org/10.1111/j.1751-8369.1992.tb00409.x

Edwards, M.B. 1976. Growth faults in upper Triassic deltaic sediments, Svalbard. *AAPG Bulletin*, **60**, 341–355.

Edwards, M.B. 1979. Sandstone in Lower Cretaceous Helvetiafjellet Formation, Svalbard: bearing on reservoir potential of the Barents shelf. *AAPG Bulletin*, **63**, 2193–2203.

Ehrenberg, S.N., Pickard, N.A.H., Henriksen, L.B., Svånå, T.A., Gutteridge, P. and McDonald, D. 2001. A depositional and sequence stratigraphic model for cold-water, spiculitic strata based on the Kapp Starostin Formation (Permian) of Spitsbergen and equivalent deposits from the Barents Sea. *AAPG Bulletin*, **85**, 2061–2087, https://doi.org/10.1306/8626D347-173B-11D7-8645000102C1865D

Eiken, O. 1985. Seismic mapping of the post-Caledonian strata in Svalbard. *Polar Research*, **3**, 167–176.

Eiken, O. 1994. *Seismic Atlas of Western Svalbard: A Selection of Regional Seismic Transects*. Norsk Polarinstitutt, Oslo.

Eliassen, A. and Talbot, M.R. 2005. Solution-collapse breccias of the Minkinfjellet and Wordiekammen Formations, Central Spitsbergen, Svalbard: a large gypsum palaeokarst system. *Sedimentology*, **52**, 775–794, https://doi.org/10.1111/j.1365-3091.2005.00731.x

Embry, A.F. 1997. Global sequence boundaries of the Triassic and their recognition in the western Canada Sedimentary Basin. *Bulletin of Canadian Petroleum Geology*, **45**, 415–433.

Embry, A.F. 2009. *Practical Sequence Stratigraphy*. Canadian Society of Petroleum Geologists.

Faleide, J.I., Tsikalas, F. *et al*. 2008. Structure and evolution of the continental margin off Norway and the Barents Sea. *Episodes*, **31**, 82–91, https://doi.org/10.18814/epiiugs/2008/v31i1/012

Faleide, J.I., Pease, V. *et al*. 2017. Tectonic implications of the lithospheric structure across the Barents and Kara shelves. *Geological Society, London, Special Publications*, **460**, 285–314, https://doi.org/10.1144/SP460.18

Faleide, J.I., Wong, P.W., Hassaan, M., Abdelmalak, M.M., Tsikalas, F. and Gabrielsen, R.H. In review. West Barents Sheared Margin Composite Tectono-Sedimentary Element, Norwegian-Greenland Sea and Fram Strait. *Geological Society, London, Memoirs*, **57**.

Gayer, R.A., Gee, D.G., Winsnes, T.S., Harland, W,B., Wallis, R.H., Miller, J.A. and Spall, H.R. 1966. Radiometric age determinations on rocks from Spitsbergen. *Norsk Polarinstitutt Skrifter*, **137**, 4–39.

Gilmullina, A., Klausen, T.G., Paterson, N.W., Suslova, A. and Eide, C.H. 2021. Regional correlation and seismic stratigraphy of Triassic Strata in the Greater Barents Sea: implications for sediment transport in Arctic basins. *Basin Research*, **33**, 1546–1579, https://doi.org/10.1111/bre.12526

Gjelberg, J.G. and Steel, R.J. 1981. An outline of Lower–Middle Carboniferous sedimentation on Svalbard. Effects of tectonic, climatic and sea level changes in rift basin sequences. *In*: Kerr, J.W. (ed.) *Geology of the North Atlantic Borderlands*. Canadian Society of Petroleum Geology, 543–561.

Gjelberg, J. and Steel, R.J. 1995. Helvetiafjellet Formation (Barremian–Aptian) Spitsbergen: characteristics of a transgressive succession. *Norwegian Petroleum Society Special Publications*, **5**, 571–593.

Glørstad-Clark, E., Birkeland, E.P., Nystuen, J.P., Faleide, J.I. and Midtkandal, I. 2011. Triassic platform-margin deltas in the western Barents Sea. *Marine and Petroleum Geology*, **28**, 1294–1314, https://doi.org/10.1016/j.marpetgeo.2011.03.006

Gradstein, F.M. and Ogg, J.G. 2020. The chronostratigraphic scale. *In*: Gradstein, F.M., Ogg, J.G., Schmitz, M.D. and Ogg, G.M. (eds) *Geologic Time Scale*. Elsevier, Amsterdam, 21–32, https://doi.org/10.1016/B978-0-12-824360-2.00002-4

Grantz, A., Hart, P.E. and Childers, V.A. 2011. Geology and tectonic development of the Amerasia and Canada Basins, Arctic Ocean. *Geological Society, London, Memoirs*, **35**, 771–799, https://doi.org/10.1144/M35.50

Green, P.F. and Duddy, I.R. 2010. Synchronous exhumation events around the Arctic including examples from Barents Sea and Alaska North Slope. *Geological Society, London, Petroleum Geology Conference Series*, **7**, 633–644, https://doi.org/10.1144/0070633

Grogan, P., Østvedt-Ghazi, A.-M., Larssen, G.B., Fotland, B., Nyberg, K., Dahlgren, S. and Eidvin, T. 1999. Structural elements and petroleum geology of the Norwegian sector of the northern Barents Sea. *Geological Society, London, Petroleum Geology Conference Series*, **5**, 247–259, https://doi.org/10.1144/0050247

Grogan, P., Nyberg, K., Fotland, B., Myklebust, R., Dahlgren, S. and Riis, F. 2000. Cretaceous magmatism south and east of Svalbard: evidence from seismic reflection and magnetic. *Polarforschung*, **68**, 25–34.

Grundvåg, S.-A. and Olaussen, S. 2017. Sedimentology of the Lower Cretaceous at Kikutodden and Keilhaufjellet, southern

Spitsbergen: implications for an onshore–offshore link. *Polar Research*, **36**, https://doi.org/10.1080/17518369.2017.1302124

Grundvåg, S.-A., Helland-Hansen, W., Johannessen, E.P., Olsen, A.H. and Stene, S.A.K. 2014*a*. The depositional architecture and facies variability of shelf deltas in the Eocene Battfjellet Formation, Nathorst Land, Spitsbergen. *Sedimentology*, **61**, 2172–2204, https://doi.org/10.1111/sed.12131

Grundvåag, S.-A., Johannessen, E.P., Helland-Hansen, W. and Plink-Bjørklund, P. 2014*b*. Depositional architecture and evolution of progradationally stacked lobe complexes in the Eocene Central Basin of Spitsbergen. *Sedimentology*, **61**, 535–569, https://doi.org/10.1111/sed.12067

Grundvåg, S.-A., Marin, D., Kairanov, B., Śliwińska, K.K., Nøhr-Hansen, H., Escalona, A. and Olaussen, S. 2017. The Lower Cretaceous succession of the northwestern Barents Shelf: onshore and offshore correlation. *Marine and Petroleum Geology*, **86**, 834–857, https://doi.org/10.1016/j.marpetgeo.2017.06.036

Grundvåg, S.A., Jelby, M.E. *et al*. 2019. Sedimentology and palynology of the Lower Cretaceous succession of central Spitsbergen: integration of subsurface and outcrop data. *Norwegian Journal of Geology*, **99**, 253–284, https://doi.org/10.17850/njg006

Grundvåg, S.-A., Jelby, M.E., Olaussen, S. and Śliwińska, K.K. 2020. The role of shelf morphology on storm-bed variability and stratigraphic architecture, Lower Cretaceous, Svalbard. *Sedimentology*, **68**, 196–237, https://doi.org/10.1111/sed.12791

Hagset, A., Grundvåg, S.-A., Badics, B., Davies, R. and Rotevatn, A. 2022. Tracing Lower Cretaceous organic-rich units across the SW Barents Shelf. *Marine and Petroleum Geology*, **140**, 105664, https://doi.org/10.1016/j.marpetgeo.2022.105664

Haile, B.G., Klausen, T.G., Jahren, J., Braathen, A. and Hellevang, H. 2018. Thermal history of a Triassic sedimentary sequence verifiedby a multi-method approach: Edgeøya, Svalbard, Norway. *Basin Research*, **30**, 1075–1097, https://doi.org/10.1111/bre.12292

Haile, B.G., Line, L.H., Klausen, T.G., Olaussen, S., Eide, C.H., Jahren, J. and Hellevang, H. 2021. Quartz overgrowth textures and fluid inclusion thermometry evidence for basin-scale sedimentary recycling: an example from the Mesozoic Barents Sea Basin. *Basin Research*, **33**, 1697–1710, https://doi.org/10.1111/bre.12531

Haremo, P. and Andresen, A. 1992. Tertiary decollements thrusting and inversion structures along Billefjorden and Lomfjorden Fault Zones, East Central Spitsbergen. *Norwegian Petroleum Society Special Publications*, **1**, 481–494.

Harland, W.B. 1997. Svalbard. *Geological Society, London, Memoirs*, **17**, 3–15, https://doi.org/10.1144/GSL.MEM.1997.017.01.01

Harland, W.B. and Kelly, S.R.A. 1997. Eastern Svalbard Platform. *Geological Society, London, Memoirs*, **17**, 75–95, https://doi.org/10.1144/GSL.MEM.1997.017.01.05

Helland-Hansen, W. 1990. Sedimentation in a Paleogene foreland basin,Spitsbergen. *AAPG Bulletin*, **74**, 260–272.

Helland-Hansen, W. 2010. Facies and stacking patterns of shelf-deltas within the Palaeogene Battfjellet Formation, NordenskiöldLand, Svalbard: implications for subsurface reservoir prediction. *Sedimentology*, **57**, 190–208, https://doi.org/10.1111/j.1365-3091.2009.01102.x

Helland-Hansen, W. and Grundvåg, S.A. 2020. The Svalbard Eocene–Oligocene (?) Central Basin succession: sedimentation patterns and controls. *Basin Research*, **33**, 729–753, https://doi.org/10.1111/bre.12492

Hellem, T. 1980. *En Sedimntologisk og Diagenetisk Undersøkelse av av Utvalgte Profiler fra Tempekfjorden Gruppen i Isfjorden Området Spitsbergen*. Master's thesis, Universitete i Oslo, Oslo, Norway.

Hellman, F.J., Gee, D.G. and Witt-Nilsson, P. 2001. Late Archean basement in the Bangenhuken Complex of the Nordbreen Nappe, western Ny-Friesland, Svalbard. *Polar Research*, **20**, 49–59, https://doi.org/10.3402/polar.v20i1.6499

Henriksen, E., Bjørnseth, H. *et al*. 2011*a*. Uplift and erosion of the greater Barents Sea: impact on prospectivity and petroleum systems. *Geological Society, London, Memoirs*, **35**, 271–281, https://doi.org/10.1144/M35.17

Henriksen, E., Ryseth, A.E., Larssen, G.B., Heide, T., Rønning, K., Sollid, K. and Stoupakova, A.V. 2011*b*. Tectonostratigraphy of the greater Barents Sea: implications for petroleum systems. *Geological Society, London, Memoirs*, **35**, 163–195, https://doi.org/10.1144/M35.10

Hjelstuen, B.O., Elverhøi, A. and Faleide, J.I. 1996. Cenozoic erosion and sediment yield in the drainage area of the Storfjorden Fan. *Global Planetary Change*, **12**, 95–117, https://doi.org/10.1016/0921-8181(95)00014-3

Hodson, A.J., Nowak, A. *et al*. 2020. Open system pingos as hotspots for sub-permafrost methane emission in Svalbard. *The Cryosphere*, **14**, 3829–3842, https://doi.org/10.5194/tc-14-3829-2020

Holliday, D. and Cutbill, J. 1972. The Ebbadalen Formation (Carboniferous), Spitsbergen. *Proceedings of the Yorkshire Geological Society*, **39**, 1–32, https://doi.org/10.1144/pygs.39.1.1

Hounslow, M.W., Harris, S.E., Karloukovski, V. and Mørk, A. 2022. Geomagnetic polarity and carbon isotopic stratigraphic assessment of the late Carnian-earliest Norian in Svalbard: evidence for a major hiatus and improved Boreal to Tethyan correlation. *Norwegian Journal of Geology*, **102**, 202204, https://doi.org/10.17850/njg102-1-4

Høy, T. and Lundschien, B.A. 2011. Triassic deltaic sequences in the northern Barents Sea. *Geological Society, London, Memoirs*, **35**, 249–260, https://doi.org/10.1144/M35.15

Hvoslef, S., Dypvik, H. and Solli, H. 1986. A combined sedimentological and organic geochemical study of the Jurassic/Cretaceous Janusfjellet Formation (Svalbard), Norway. *Organic Geochemistry*, **10**, 101–111, https://doi.org/10.1016/0146-6380(86)90013-6

Ingólfsson, Ó. and Landvik, J.Y. 2013. The Svalbard–Barents Sea ice-sheet – historical, current and future perspectives. *Quaternary Scence Review*, **64**, 33–60, https://doi.org/10.1016/j.quascirev.2012.11.034

Jelby, M.E., Grundvåg, S.-A., Helland-Hansen, W., Olaussen, S. and Stemmerik, L. 2020. Tempestite facies variability and storm-depositional processes across a wide ramp: towards a polygenetic model for hummocky cross-stratification. *Sedimentology*, **67**, 742–781, https://doi.org/10.1111/sed.12671

Jochmann, M.M., Brugmans, P., Often, M., Friis, B. and Holst, B. 2015. Coal resources on Svalbard – status, geology, and challenges. Presented at the Geological Survey of Norway 31st Winter Conference, 12–14 January 2015, Stavanger, Norway, https://doi.org/10.13140/RG.2.2.35848.29449

Jochmann, M.M., Augland, L.E. *et al*. 2020. Sylfjellet: a new outcrop of the Paleogene Van Mijenfjorden Group in Svalbard. *Arktos*, **6**, 17–38, https://doi.org/10.1007/s41063-019-00072-w

Johannessen, E.P. and Steel, R. 1992. Mid-Carboniferous extension and rift-infill sequences in the Billefjorden Trough, Svalbard. *Norsk Geologisk Tidsskrift*, **72**, 35–48.

Johannessen, E.P., Henningsen, T. *et al*. 2011. Palaeogene clinoform succession on Svalbard expressed in outcrops, seismic data, logs and cores. *First Break*, **29**, 35–44, https://doi.org/10.3997/1365-2397.2011004

Johansen, T.A., Digranes, P., van Schaack, M. and Lønne, I. 2003. Seismic mapping and modeling of near-surface sediments in polar areas. *Geophysics*, **68**, 566–573, https://doi.org/10.1190/1.1567226

Johansen, T.A., Ruud, B.O., Bakke, N.E., Riste, P., Johannessen, E.P. and Henningsen, T. 2011. Seismic profiling on Arctic glaciers. *First Break*, **29**, 65–71, https://doi.org/10.3997/1365-2397.20112st1

Jones, M.T., Eliassen, G.T. *et al*. 2016. Provenance of bentonite layers in the Palaeocene strata of the Central Basin, Svalbard: implications for magmatism and rifting events around the onset of the North Atlantic Igneous Province. *Journal of Volcanology and Geothermal Research*, **327**, 571–584, https://doi.org/10.1016/j.jvolgeores.2016.09.014

Jones, M.T., Augland, L.E. *et al*. 2017. Constraining shifts in North Atlantic plate motions during the Palaeocene by U–Pb dating

of Svalbard tephra layers. *Scientific Reports*, **7**, 6822, https://doi.org/10.1038/s41598-017-06170-7

Kierulf, H.P., Kohler, J. *et al*. 2022. Time-varying uplift in Svalbard – an effect of glacial changes. *Geophysical Journal International*, **231**, 1518–1534, https://doi.org/10.1093/gji/ggac264

Klausen, T.G. and Mørk, A. 2014. Upper Triassic paralic deposits of the De Geerdalen Formation on Hopen: outcrop analog to the subsurface Snadd Formation in the Barents Sea. *AAPG Bulletin*, **98**, 1911–1941, https://doi.org/10.1306/0219141 3064

Klausen, T.G., Ryseth, A.E., Helland-Hansen, W., Gawthorpe, R. and Laursen, I. 2014. Spatial and temporal changes in geometries of fluvial channel bodies from the Triassic Snadd Formation of offshore Norway. *Journal of Sedimentary Research*, **84**, 567–585, https://doi.org/10.2110/jsr.2014.47

Klausen, T.G., Torland, J.A., Eide, C.H., Alaei, B., Olaussen, S. and Chiarella, D. 2017. Clinoform development and topset evolution in a mud-rich delta – the Triassic Kobbe Formation, Norwegian Barents Sea. *Sedimentology*, **65**, 1132–1169, https://doi.org/10.1111/sed.12417

Klausen, T.G., Nyberg, B. and Helland-Hansen, W. 2019. The largest delta plain in Earth's history. *Geology*, **47**, 470–474, https://doi.org/10.1130/G45507.1

Klausen, T.G., Rismyhr, B., Müller, R. and Olaussen, S. 2022. Changing provenance and stratigraphic signatures across the Triassic–Jurassic boundary in eastern Spitsbergen and the subsurface Barents Sea. *Norwegian Journal of Geology*, **102**, 202205, https://dx.doi.org/10.17850/njg102-2-1

Knag, G. 1980. *Gipshuken-og Kapp Starostin Formasjonene Mellom til Øvre Perm, Langs Vestkysten av Svalbard*. Master's thesis, Universitetet i Begen Geologisk Institutt, Bergen, Norway.

Knies, J., Matthiessen, J. *et al*. 2009. The Plio-Pleistocene glaciation of the Barents Sea–Svalbard region: a new model based on revised chronostratigraphy. *Quaternary Science Reviews*, **28**, 812–829, https://doi.org/10.1016/j.quascirev.2008.12.002

Koevoets, M.J., Abay, T.B., Hammer, Ø. and Olaussen, S. 2016. High-resolution organic carbon-isotope stratigraphy of the Middle Jurassic–Lower Cretaceous Agardhfjellet Formation of Central Spitsbergen, Svalbard. *Palaeogeography, Palaeoclimatology, Palaeoecology*, **449**, 266–274, https://doi.org/10.1016/j.palaeo.2016.02.029

Koevoets, M.J., Hammer, Ø., Olaussen, S., Senger, K. and Smelror, M. 2018. Integrating subsurface and outcrop data of the Middle Jurassic to Lower Cretaceous Agardfjellet Formation in central Spitsbergen. *Norwegian Journal of Geology*, **99**, 219–252, https://doi.org/10.17850/njg98-4-01

Krajewski, K.P. and Weitschat, W. 2015. Depositional history of the youngest strata of the Sassendalen Group (Bravaisberget Formation, Middle Triassic–Carnian) in southern Spitsbergen, Svalbard. *Annales Societatis Geologorum Poloniae*, **85**, 151–175, https://doi.org/10.14241/asgp.2014.005

Krajewski, K.P. 2013. Organic matter–apatite–pyrite relationships in the Botneheia Formation (Middle Triassic) of eastern Svalbard: relevance to the formation of petroleum source rocks in the NW Barents Sea shelf. *Marine and Petroleum Geology*, **45**, 69–105, https://doi.org/10.1016/j.marpetgeo.2013.04.016

Krasil'shchikov, A.A. 1964. New data on the geology of the northern part of the Spitsbergen Archipelago. *In*: Sokolov, V.N. (ed.) *Conference on the Geology of Spitsbergen, Leningrad, 1964: Summary of Contributions*. NIIGA, Leningrad, USSR, 23–25.

Larssen, G.B., Elvebakk, G. *et al*. 2002. *Upper Palaeozoic Lithostratigraphy of the Southern Part of the Norwegian Barents Sea*. Norwegian Geological Survey Bulletin, **44**.

Lasabuda, A., Geissler, W.H., Laberg, J.S., Knutsen, S.-M., Rydningen, T.A. and Berglar, K. 2018. Late Cenozoic erosion estimates for the northern Barents Sea: quantifying glacial sediment input to the Arctic Ocean. *Geochemistry, Geophysics, Geosystems*, **19**, 4876–4903, https://doi.org/10.1029/2018GC00 7882

Lasabuda, A., Johansen, N.S. *et al*. 2021. Cenozoic uplift and erosion of the Norwegian Barents Shelf – a review. *Earth-Science Reviews*, **217**, 103609, https://doi.org/10.1016/j.earscirev.2021.103609

Leever, K.A., Gabrielsen, R.H., Faleide, J.I. and Braathen, A. 2011. A transpressional origin for the West Spitsbergen fold-and-thrust belt: Insight from analog modeling. *Tectonics*, **30**, TC2014, https://doi.org/10.1029/2010TC002753

Leith, T.L., Weiss, H.M. *et al*. 1993. Mesozoic hydrocarbon source-rocks of the Arctic region. *Norwegian Petroleum Society (NPF) Special Publications*, **2**, 1–25.

Lopes, G., Mangerud, G. and Clayton, G. 2018. The palynostratigraphy of the Mississippian Birger Johnsonfjellet section, Spitsbergen, Svalbard. *Palynology*, **43**, 631–649, https://doi.org/10.1080/01916122.2018.1518849

Lord, G.S., Mørk, A. *et al*. 2022. Stratigraphy and palaeosol profiles of the Upper Triassic Isfjorden Member, Svalbard. *Norwegian Journal of Geology*, **102**, 202215, https://doi.org/10.17850/njg102-4-2

Lord, G.S., Solvi, K.H., Ask, M., Mørk, A., Hounslow, M.W. and Paterson, N.W. 2014. The Hopen Member: a new lithostratigraphic unit on Hopen and equivalent to the Isfjorden Member of Spitsbergen. *Norwegian Petroleum Bulletin*, **11**, 81–96.

Lord, G.S., Johansen, S.K., Støen, S.J. and Mørk, A. 2017. Facies development of the Upper Triassic succession on Barentsøya, Wilhelmøya and NE Spitsbergen, Svalbard. *Norwegian Journal of Geology*, **97**, 33–62, https://doi.org/10.17850/njg97-1-03

Lord, G.S., Mørk, M.B.E., Mørk, A. and Olaussen, S. 2019. Sedimentology and petrography of the Svenskøya Formation on Hopen, Svalbard: an analogue to sandstone reservoirs in the Realgrunnen Subgroup. *Polar Research*, **38**, https://doi.org/10.33265/polar.v38.3523

Lucazeau, F. 2019. Analysis and mapping of an updated terrestrial heat flow data set. *Geochemistry, Geophysics, Geosystems*, **20**, 4001–4024, https://doi.org/10.1029/2019GC008389

Lundschien, B.A., Høy, T. and Mørk, A. 2014. Triassic hydrocarbon potential in the Northern Barents Sea; integrating Svalbard and stratigraphic core data. *Norwegian Petroleum Directorate Bulletin*, **11**, 3–20.

Lundschien, B.A., Mattingsdal, R., Johansen, S.K. and Knutsen, S.M. 2023. North Barents Composite Tectono-Sedimentary Element. *Geological Society, London, Memoirs*, **57**, https://doi.org/10.1144/M57-2021-39

Lüthje, C.J., Nichols, G. and Jerrett, R. 2020. Sedimentary facies and reconstruction of a transgressive coastal plain with coal formation, Paleocene, Spitsbergen, Arctic Norway. *Norwegian Journal of Geology*, **100**, 202010, https://dx.doi.org/10.17850/njg100-2-1

Maher, H.D. Jr 2001. Manifestations of the Cretaceous High Arctic Large Igneous Province in Svalbard. *The Journal of Geology*, **109**, 91–104, https://doi.org/10.1086/317960

Maher, H., Senger, K., Braathen, A., Mulrooney, M. J., Smyrak-Sikora, A., Osmundsen, P. T. and Ogata, K. 2020. Mesozoic-Cenozoic regional stress field evolution in Svalbard. *Tectonics*, **39**, e2018TC005461, https://doi.org/10.1029/2018TC005461

Maher, H.D. Jr and Braathen, A. 2011. Løvehovden fault and Billefjorden rift basin segmentation and development, Spitsbergen, Norway. *Geological Magazine*, **148**, 154–170, https://doi.org/10.1017/S0016756810000567

Maher, H.D. Jr, Bergh, S.G., Braathen, A. and Ohta, Y. 1997. Svartfjella, Eidembukta, and Daudmannsodden lineament – decoupled orogen-parallel motion in the crystalline hinterland of Spitsbergen's fold-thrust belt. *Tectonics*, **16**, 88–106, https://doi.org/10.1029/96TC02616

Maher, H.D., Jr, Hays, T., Shuster, R. and Mutrux, J. 2004. Petrography of the Lower Cretaceous sandstones of Spitsbergen. *Polar Research*, **23**, 147–165, https://doi.org/10.3402/polar.v23i2.6276

Marshall, C., Uguna, J. *et al*. 2015. Geochemistry and petrology of Palaeocene coals from Spitzbergen – Part 2: maturity variations and implications for local and regional burial models. *International Journal of Coal Geology*, **143**, 1–10, https://doi.org/10.1016/j.coal.2015.03.013

Matysik, M., Stemmerik, L., Olaussen, S. and Brunstad, H. 2017. Diagenesis of spiculites and carbonates in a Permian temperate ramp succession, Tempelfjorden Group, Spitsbergen, Arctic

Norway. *Sedimentology*, **65**, 745–774, https://doi.org/10.1111/sed.12404

McCann, A.J. and Dallmann, W.K. 1996. Reactivation history of the long-lived Billefjorden Fault Zone in north central Spitzbergen, Svalbard. *Geological Magazine*, **133**, 63–84, https://doi.org/10.1017/S0016756800007251

Midtkandal, I. and Nystuen, J.P. 2009. Depositional architecture of a low-gradient ramp shelf in an epicontinental sea: the lower Cretaceous of Svalbard. *Basin Research*, **21**, 655–675, https://doi.org/10.1111/j.1365-2117.2009.00399.x

Midtkandal, I., Nystuen, J.P., Nagy, J. and Mørk, A. 2008. Lower Cretaceous lithostratigraphy across a regional subaerial unconformity in Spitsbergen: the Rurikfjellet and Helvetiafjellet formations. *Norwegian Journal of Geology*, **88**, 287–304.

Midtkandal, I., Svensen, H. *et al*. 2016. The Aptian oceanic anoxic event (OAE1a) in Svalbard and the age of the Barremian–Aptian boundary. *Palaeogeography, Palaeoclimatology, Palaeoecology*, **463**, 126–135, https://doi.org/10.1016/j.palaeo.2016.09.023

Minakov, A. 2018. Late Cenozoic lithosphere dynamics in Svalbard: interplay of glaciation, seafloor spreading and mantle convection. *Journal of Geodynamics*, **122**, 1–16, https://doi.org/10.1016/j.jog.2018.09.009

Mørk, A. and Bjorøy, M. 1984. Mesozoic source rocks on Svalbard. *In*: Spencer, A.M. (ed.) *Petroleum Geology of the North European Margin*. Springer, Dordrecht, The Netherlands, 371–382, https://doi.org/10.1007/978-94-009-5626-1_28

Mørk, A., Knarud, R. and Worsley, D. 1982. Depositional and diagenetic environments of the Triassic and Lower Jurassic succession of Svalbard. *Canadian Society of Petroleum Geologists Memoirs*, **8**, 371–398.

Mørk, A., Dallmann, W.K. *et al*. 1999. Mesozoic lithostratigraphy. *In*: Dallmann, W.K., Birkenmajer, K. *et al*. eds 1999. *Lithostratigraphic Lexicon of Svalbard. Review and Recommendations for Nomenclature Use; Upper Palaeozoic to Quaternary Bedrock*. Norsk Polarinstitutt, Tromsø, Norway, 127–214.

Mørk, M.B.E. 2013. Diagenesis and quartz cement distribution of low permeability Upper Triassic–Middle Jurassic reservoir sandstones, Longyearbyen CO_2 laboratory well site in Svalbard, Norway. *AAPG Bulletin*, **97**, 577–596, https://doi.org/10.1306/10031211193

Müller, R., Klausen, T.G., Faleide, J.I., Olaussen, S., Eide, C.H. and Suslova, A. 2019. Linking regional unconformities in the Barents Sea to compression-induced forebulge uplift at the Triassic–Jurassic transition. *Tectonophysics*, **765**, 35–51, https://doi.org/10.1016/j.tecto.2019.04.006

Mulrooney, M.J., Rismyhr, B., Yenwongfai, H.D., Leutscher, J., Olaussen, S. and Braathen, A. 2018. Impacts of small-scale faults on continental to coastal plain deposition: evidence from the Realgrunnen Subgroup in the Goliat field, southwest Barents Sea, Norway. *Marine and Petroleum Geology*, **95**, 276–302, https://doi.org/10.1016/j.marpetgeo.2018.04.023

Nagy, J., Reolid, M. and Rodriguez-Tovar, F.J. 2009. Foraminiferal morphogroups in dysoxic shelf deposits from the Jurassic of Spitsbergen. *Polar Research*, **28**, 214–221, https://doi.org/10.3402/polar.v28i2.6119

Nasuti, A., Roberts, D. and Gernigon, L. 2015. Multiphase mafic dykes in the Caledonides of northern Finnmark revealed by a new high-resolution aeromagnetic dataset. *Norwegian Journal of Geology*, **95**, 285–297, http://doi.org/10.17850/njg95-3-02

Nemec, W., Steel, R.J., Gjelberg, J., Collinson, J.D., Prestholm, E. and Øxnevad, I.E. 1988. Anatomy of collapsed and re-established delta front in Lower Cretaceous of eastern Spitsbergen: gravitational sliding and sedimentation processes. *AAPG Bulletin*, **72**, 454–476.

Nicolaisen, J.B., Elvebakk, G. *et al*. 2019. Characterization of Upper Palaeozoic organic-rich units in Svalbard – implications for the Norwegian Barents Shelf. *Journal of Petroleum Geology*, **42**, 59–78, https://doi.org/10.1111/jpg.12724

Nøttvedt, A. 1985. Askeladden Delta Sequence (Palaeocene) on Spitsbergen – sedimentation and controls on delta formation. *Polar Research*, **3**, 21–48, https://doi.org/10.3402/polar.v3i1.6938

Nøttvedt, A., Cecchi, M. *et al*. 1993. Svalbard–Barents Sea correlation: a short review. *Norwegian Petroleum Society Special Publications*, **2**, 363–375.

Nyland, B., Jensen, L., Skagen, J., Skarpnes, O. and Vorren, T. 1992. Tertiary uplift and erosion in the Barents Sea: magnitude, timing and consequences. *Norwegian Petroleum Society Special Publications*, **1**, 153–162, https://doi.org/10.1016/B978-0-444-88607-1.50015-2

Ogata, K., Senger, K., Braathen, A., Tveranger, J. and Olaussen, S. 2012. The importance of natural fractures in a tight reservoir for potential CO_2 storage: a case study of the upper Triassic–middle Jurassic Kapp Toscana Group (Spitsbergen, Arctic Norway). *Geological Society, London, Special Publications*, **374**, 395–415, https://doi.org/10.1144/SP374.9

Ogata, K., Senger, K., Braathen, A., Tveranger, J. and Olaussen, S. 2014. Fracture systems and meso-scale structural patterns in the siliciclastic Mesozoic reservoir–caprock succession of the Longyearbyen CO_2 Lab project: implications for geologic CO_2 sequestration on Central Spitsbergen, Svalbard. *Norwegian Journal of Geology*, **94**, 121–154.

Ohm, S.E., Karlsen, D.A. and Austin, T.J.F. 2008. Geochemically driven exploration models in uplifted areas: examples from the Norwegian Barents Sea. *AAPG Bulletin*, **92**, 1191–1223, https://doi.org/10.1306/06180808028

Ohm, S.E., Larsen, L. *et al*. 2019. Discovery of shale gas in organic-rich Jurassic successions, Adventdalen, Central Spitsbergen, Norway. *Norwegian Journal of Geology*, **99**, 349–376, https://doi.org/10.17850/njg007

Olaussen, S., Larssen, G.B. *et al*. 2018. Mesozoic strata of Kong Karls Land, Svalbard, Norway; a link to the northern Barents Sea basins and platforms. *Norwegian Journal of Geology*, **98**, 1–69, https://doi.org/10.17850/njg98-4-06

Olaussen, S., Senger, K., Braathen, A., Grundvåg, S.A. and Mørk, A. 2019. You learn as long as you drill; research synthesis from the Longyearbyen CO_2 Laboratory, Svalbard, Norway. *Norwegian Journal of Geology*, **99**, 157–188, https://doi.org/10.17850/njg008

Onderdonk, N. and Midtkandal, I. 2010. Mechanisms of collapse of the Cretaceous Helvetiafjellet Formation at Kvalvågen, eastern Spitsbergen. *Marine and Petroleum Geology*, **27**, 2118–2140, https://doi.org/10.1016/j.marpetgeo.2010.09.004

Orheim, A., Bieg, G., Brekke, T., Horseide, V. and Stenvold, J. 2007. Petrography and geochemical affinities of Spitsbergen Paleocene coals, Norway. *International Journal of Coal Geology*, **70**, 116–136, https://doi.org/10.1016/j.coal.2006.04.008

Orvin, A.K. 1934. *Geology of the Kings Bay Region, Spitsbergen: With Special Reference to the Coal Deposits. Norges Svalbard-og Ishavsundersøkelser, Oslo*. Skrifter om Svalbard og Ishavet, **57**.

Paterson, N.W., Mangerud, G., Cetean, C.G., Mørk, A., Lord, G.S., Klausen, T.G. and Mørkved, P.T. 2016. A multidisciplinary biofacies characterisation of the Late Triassic (late Carnian–Rhaetian) Kapp Toscana Group on Hopen, Arctic Norway. *Palaeogeography, Palaeoclimatology, Palaeoecology*, **464**, 16–42, https://doi.org/10.1016/j.palaeo.2015.10.035

Paulsen, R.S., Birchall, T., Senger, K. and Grundvåg, S.-A. 2022. Seal characterization and integrity in uplifted basins: insights from the northern Barents Shelf. *Marine and Petroleum Geology*, **139**, 105588, https://doi.org/10.1016/j.marpetgeo.2022.105588

Petersen, T.G., Thomsen, T.B., Olaussen, S. and Stemmerik, L. 2016. Provenance shifts in an evolving Eurekan foreland basin: the Tertiary Central Basin, Spitsbergen. *Journal of the Geological Society, London*, **173**, 634–648, https://doi.org/10.1144/jgs2015-076

Piepjohn, K., von Gosen, W. and Tessensohn, F. 2016. The Eurekan deformation in theArctic: an outline. *Journal of the Geological Society, London*, **173**, 1007–1024, https://doi.org/10.1144/jgs2016-081

Polteau, S., Hendriks, B.W.H. *et al*. 2016. The Early Cretaceous Barents Sea Sill Complex: distribution, $^{40}Ar/^{39}Ar$ geochronology, and implications for carbon gas formation.

Palaeogeography Palaeoclimatology Palaeoecology, **441**, 83–95, https://doi.org/10.1016/j.palaeo.2015.07.007

Riis, F. and Fjeldskaar, W. 1992. On the magnitude of the Late Tertiary and Quaternary erosion and its significance for the uplift of Scandinavia and the Barents Sea. *Norwegian Petroleum Society Special Publications*, **1**, 163–185, https://doi.org/10.1016/B978-0-444-88607-1.50016-4

Riis, F., Lundschien, B.A., Høy, T., Mørk, A. and Mørk, M.B.E. 2008. Evolution of the Triassic shelf in the northern Barents Sea region. *Polar Research*, **27**, 318–338, https://doi.org/10.1111/j.1751-8369.2008.00086.x

Rismyhr, B., Bjærke, T., Olaussen, S., Mulrooney, M.J. and Senger, K. 2018. Facies, palynostratigraphy and sequence stratigraphy of the Wilhelmøya Subgroup (Upper Triassic–Middle Jurassic) in western central Spitsbergen, Svalbard. *Norwegian Journal of Geology*, **99**, 189–218, https://doi.org/10.17850/njg001

Rød, R.S., Hynne, I.B. and Mørk, A. 2014. Depositional environment of the Upper Triassic De Geerdalen Formation – an EW transect from Edgeøya to Central Spitsbergen, Svalbard. *Norwegian Petroleum Directorate Bulletin*, **11**, 21–40.

Roy, S., Hovland, M., Noormets, R. and Olaussen, S. 2015. Seepage in Isfjorden and its tributary fjords, west Spitsbergen. *Marine Geology*, **363**, 146–159, https://doi.org/10.1016/j.margeo.2015.02.003

Roy, S., Senger, K., Hovland, M., Römer, M. and Braathen, A. 2019. Geological controls on shallow gas distribution and seafloor seepage in an Arctic fjord of Spitsbergen, Norway. *Marine and Petroleum Geology*, **107**, 237–254, https://doi.org/10.1016/j.marpetgeo.2019.05.021

Ryseth, A. 2014. Sedimentation at the Jurassic–Triassic boundary, south-west Barents Sea: indication of climate change. *International Association of Sedimentologists Special Publications*, **46**, 187–214, https://doi.org/10.1002/9781118920435.ch9

Schaaf, N.W., Osmundsen, P.T., Van der Lelij, R., Schönenberger, J., Lenz, O.K., Redfield, T. and Senger, K. 2021. Tectono-sedimentary evolution of the eastern Forlandsundet Graben, Svalbard. *Norwegian Journal of Geology*, **100**, 202021, https://doi.org/10.17850/njg100-4-4

Seidler, L., Steel, R.J., Stemmerik, L. and Surlyk, F. 2004. North Atlantic marine rifting in the Early Triassic: new evidence from East Greenland. *Journal of the Geological Society, London*, **161**, 583–592, https://doi.org/10.1144/0016-764903-063

Senger, K., Roy, S. *et al*. 2013. Geometries of doleritic intrusions in central Spitsbergen, Svalbard: an integrated study of an onshore–offshore magmatic province with implications for CO_2 sequestration. *Norwegian Journal of Geology*, **93**, 143–166.

Senger, K., Planke, S., Polteau, S., Ogata, K. and Svensn, H. 2014*a*. Sill emplacement and contact metamorphism in a siliciclastoic reservoir on Svalbard, Arctic Norway. *Norwegian Journal of Geology*, **94**, 155–169.

Senger, K., Tveranger, J., Ogata, K., Braathen, A. and Planke, S. 2014*b*. Late Mesozoic magmatism in Svalbard: a review. *Earth-Science Reviews*, **139**, 123–144, https://doi.org/10.1016/j.earscirev.2014.09.002

Senger, K., Tveranger, J., Braathen, A., Ogata, K., Olaussen, S. and Larsen, L. 2015. CO_2 storage resource estimates in unconventional reservoirs: insights from a pilot-sized storage site in Svalbard, Arctic Norway. *Environmental Earth Sciences*, **73**, 3987–4009, https://doi.org/10.1007/s12665-014-3684-9

Senger, K., Brugmans, P. *et al*. 2019. Petroleum, coal and research drilling onshore Svalbard: a historical perspective. *Norwegian Journal of Geology*, **99**, 1–30, https://doi.org/10.17850/njg99-3-1

Senger, K., Betlem, P. *et al*. 2021. Using digital outcrops to make the high Arctic more accessible through the Svalbox database. *Journal of Geoscience Education*, **69**, 123–137, https://doi.org/10.1080/10899995.2020.1813865

Śliwińska, K.K., Jelby, M.E., Grundvåg, S.-A., Nøhr-Hansen, H., Alsen, P. and Olaussen, S. 2020. Dinocyst stratigraphy of the Valanginian to Aptian succession (the Rurikfjellet and Helvetiafjellet formations) from Spitsbergen, Norway. *Geological Magazine*, **57**, 1693–1714, https://doi.org/10.1017/S0016756819001249

Smelror, M. and Larssen, G.B. 2016. Are there Upper Cretaceous sedimentary rocks preserved on Sørkapp Land, Svalbard? *Norwegian Journal of Geology*, **96**, 147–158, https://doi.org/10.17850/njg96-2-05

Smelror, M., Mørk, A., Monteil, E., Rutledge, D. and Leereveld, H. 1998. The Klippfisk Formation – a new lithostratigraphic unit of Lower Cretaceous platform carbonates on the Western Barents Shelf. *Polar Research*, **17**, 181–202.

Smelror, M., Petrov, O.V., Larssen, G.B. and Werner, S. 2009. *Geological History of the Barents Sea*. Geological Survey of Norway, Trondheim, Norway.

Smelror, M., Larssen, G.B., Olaussen, S., Rømuld, A. and Williams, R. 2018. Late Triassic to Early Cretaceous palynostratigraphy of Kong Karls Land, Svalbard, Arctic Norway, with correlations to Franz Josef Land, Arctic Russia. *Norwegian Journal of Geology*, **98**, 1–31, https://doi.org/10.17850/njg004

Smith, D.G., Harland, W.B., Hughes, N.F. and Pickton, C.A.G. 1976. The geology of Kong Karls Land, Svalbard. *Geological Magazine*, **113**, 193–232, https://doi.org/10.1017/S001675680004320X

Smyrak-Sikora, A., Johannessen, E.P., Olaussen, S., Sandal, G. and Braathen, A. 2019. Sedimentary architecture during rift initiation – the arid Billefjorden Trough, Svalbard. *Journal of the Geological Society, London*, **176**, 225–252, https://doi.org/10.1144/jgs2018-100

Smyrak-Sikora, A., Osmundsen, P.T. *et al*. 2020. Architecture of growth basins in a tidally influenced, prodelta to delta-front setting: the Triassic succession of Kvalpynten, East Svalbard. *Basin Research*, **32**, 949–978, https://doi.org/10.1111/bre.12410

Smyrak-Sikora, A., Nicolaisen, J.B., Braathen, A., Johannessen, E.P., Olaussen, S. and Stemmerik, L. 2021. Impact of growth faults on mixed siliciclastic-carbonate–evaporite deposits during rift climax and reorganisation – Billefjorden Trough, Svalbard, Norway. *Basin Research*, **33**, 2643–2674, https://doi.org/10.1111/bre.12578

Sorento, T., Olaussen, S. and Stemmerik, L. 2020. Controls on deposition of shallow marine carbonates and evaporates – lower Permian Gipshuken Formation, Central Spitsbergen, Arctic Norway. *Sedimentology*, **67**, 207–238, https://doi.org/10.1111/sed.12640

Spychala, Y.T., Ramaaker, T.A.B., Eggenhuisen, J.T., Grundvåg, S.-A., Pohl, F. and Wróblewska, S. 2021. Proximal to distal grain-size distribution of basin-floor lobes: A study from the Battfjellet Formation, Central Tertiary Basin, Svalbard. *The Depositional Record*, **8**, 436–456, https://doi.org/10.1002/dep2.167

Steel, R.J. and Gjelberg, J. 1981. An outline of Lower–Middle Carboniferous sedimentation on Svalbard: effects of tectonic, climatic and sea level changes in rift basin sequences. *Canadian Society of Petroleum Geologists Memoirs*, **7**, 543–561.

Steel, R.J. and Worsley, D. 1984. Svalbard's post-Caledonian strata – an atlas of sedimentation patterns and palaeogeographic evolution. *In*: Spencer, A.M. (ed.) *Petroleum Geology of the North European Margin*. Springer, Dordrecht, The Netherlands, 109–135.

Steel, R.J., Dalland, A., Kalgraff, K. and Larsen, V. 1981. The Central Tertiary Basin of Spitsbergen: sedimentary development of a sheared margin basin. *Canadian Society of Petroleum Geologists Memoirs*, **7**, 647–664.

Steel, R.J., Gjelberg, J., Helland-Hansen, W., Kleinspehn, K., Nøttvedt, A. and Rye-Larsen, M. 1985. The Tertiary strike-slip basins and orogenic belt of Spitsbergen. *SEPM Special Publications*, **37**, 339–359.

Stemmerik, L. and Worsley, D. 1995. Permian history of the Barents Shelf area. *In*: Scholle, P.A., Peryt, T.M. and Ulmer-Scholle, D.S. (eds) *Permian of Northern Pangaea, Volume 2*. Springer, Berlin, 81–97.

Stemmerik, L. and Worsley, D. 2005. 30 years on – Arctic Upper Palaeozoic stratigraphy, depositional evolution and hydrocarbon prospectivity. *Norwegian Journal of Geology*, **85**, 151–168.

Throndsen, T. 1982. Vitrinite reflectance studies of coals and dispersedorganic matter in Tertiary deposits in the Adventdalen area, Svalbard. *Polar Research*, **2**, 77–91.

Tsikalas, F., Blaich, O.A., Faleide, J.I. and Olaussen, S. 2021. Stappen High–Bjørnøya Tectono-Sedimentary Element, Barents Sea. *Geological Society, London, Memoirs*, **57**, https://doi.org/10.1144/M57-2016-24

Uchman, A., Hanken, N.M., Nielsen, J.K., Grundvåg, S.-A. and Piasecki, S. 2016. Depositional environment, ichnological features and oxygenation of Permian to earliest Triassic marine sediments in central Spitsbergen, Svalbard. *Polar Research*, **35**, https://doi.org/10.3402/polar.v35.24782

van Koeverden, J.H., Karlsen, D.A. and Backer-Owe, K. 2011. Carboniferous non-marine source rocks from Spitsbergen and Bjørnøya: comparison with the Western Arctic. *Journal of Petroleum Geology*, **34**, 53–66, https://doi.org/10.1111/j.1747-5457.2011.00493.x

Uguna, J.O., Carr, A.D. *et al*. 2017. Improving spatial predictability of petroleum resources within the Central Tertiary Basin, Spitsbergen: a geochemical and petrographic study of coals from the eastern and western coalfields. *International Journal of Coal Geology*, **179**, 278–294, https://doi.org/10.1016/j.coal.2017.06.007

van Koeverden, J.H. and Karlsen, D.A. 2011. Carboniferous non-marine source rocks from Svalbard and Bjørnøya: comparison with the Western Arctic. *Journal of Petroleum Geology*, **34**, 53–66, https://doi.org/10.1111/j.1747-5457.2011.00493.x

Vigran, J.O., Mangerud, G., Mørk, A., Worsley, D. and Hochuli, P.A. 2014. *Palynology and Geology of the Triassic Succession of Svalbard and the Barents Sea*. Geological Survey of Norway Special Publications, **14**.

Walderhaug, O. 1996. Kinetic modeling of quartz cementation and porosity loss in deeply buried sandstone reservoirs. *AAPG Bulletin*, **80**, 731–745.

Wangen, M., Souche, A. and Johansen, H. 2016. Amodel for underpressure development in a glacial valley, an example from Adventdalen. *Svalbard Basin Research*, **28**, 752–769, https://doi.org/10.1111/bre.12130

Wesenlund, F., Grundvåg, S.-A., Sjøholt, V.E., Thiessen, O. and Pedersen, J.H. 2021. Linking facies variations, organic carbon richness and bulk bitumen content – a case study from the organic-rich Middle Triassic shales of eastern Svalbard. *Marine and Petroleum Geology*, **132**, 105168, https://doi.org/10.1016/j.marpetgeo.2021.105168

Wesenlund, F., Grundvåg, S.-A., Engelschiøn, V.S., Thießen, O. and Pedersen, J.H. 2022. Multi-elemental chemostratigraphy of Triassic mudstones in eastern Svalbard: implications for source rock formation in front of the World's largest delta plain. *The Depositional Record*, **8**, 718–753, https://doi.org/10.1002/dep2.182

Worsley, D. 2008. The post-Caledonian development of Svalbard and the western Barents Sea. *Polar Research*, **27**, 298–317, https://doi.org/10.1111/j.1751-8369.2008.00085.x

Zhang, Y., Ogg, J.G., Minguez, D.A., Hounslow, M.W. and Olaussen, S. 2021. Magnetostratigraphy of U–Pb–dated boreholes in Svalbard, Norway, implies that magnetochron M0r (a proposed Barremian–Aptian boundary marker) begins at 121.2 ± 0.4 Ma. *Geology*, **49**, 733–737, https://doi.org/10.1130/G48591.1

Zuchuat, V., Sleveland, A.R.N. *et al.* 2020. A new high-resolution stratigraphic and palaeoenvironmental record spanning the End-Permian Mass Extinction and its aftermath in central Spitsbergen, Svalbard. *Palaeogeography, Palaeoclimatology, Palaeoecology*, **554**, 109732, https://doi.org/10.1016/j.palaeo.2020.109732